

Journal of Climate

CMIP5 Simulations of Low-Level Tropospheric Temperature and Moisture over tropical Americas

--Manuscript Draft--

Manuscript Number:	
Full Title:	CMIP5 Simulations of Low-Level Tropospheric Temperature and Moisture over tropical Americas
Article Type:	Article
Corresponding Author:	Leila V Carvalho, Ph.D. University of California Santa Barbara, CA UNITED STATES
Corresponding Author's Institution:	University of California
First Author:	Leila V Carvalho, Ph.D.
Order of Authors:	Leila V Carvalho, Ph.D. Charles Jones
Abstract:	<p>Global warming has been linked to systematic changes in North and South Americas climates and may severely impact the North American and South American Monsoon systems (NAMS and SAMS, respectively). Monsoon characteristics (e.g, onset, duration and seasonal amplitude) depend greatly on the magnitude and spatial extent of the land-ocean temperature contrast and atmospheric moisture content, among other factors. This study examines interannual-to-decadal variations and changes in the low-troposphere (850hPa) temperature (T850) and specific humidity (Q850) over the NAMS and SAMS using NCEP/NCAR and CFSR reanalyses and fifth phase of the Coupled Model Intercomparison Project (CMIP5) simulations for two scenarios: "historical" and high emission representative concentration pathways "RCP8.5". Trends in the magnitude and area of the 85th percentiles were distinctly examined over SAMS and NAMS regions during the peak of the respective monsoon seasons. The historical simulations (1951-2005) and the two reanalyses agree well and indicate that significant warming has occurred over tropical South America with a remarkable increase in the area and magnitude of the 85th percentile in the last decade (1996-2005). The RCP8.5 CMIP5 ensemble mean projects an increase in the T850 85th percentile of about 2.5oC (2.8oC) by 2050 and 4.8oC (5.5oC) over South America (North America) by 2095 relative to 1955. The area of South America (North America) with T850 \geq the 85th percentile is projected to increase from ~10% (15%) in 1955 to ~58% (~33%) by 2050 and ~80% (~50%) by 2095. This progressive warming is associated with an increase in the 85th percentile of Q850 of about 3g kg⁻¹ over SAMS and NAMS by 2095.</p>
Suggested Reviewers:	<p>Wayne Higgins Wayne.Higgins@noaa.gov Dr. Higgins is expert in climate variation and changes in the North America and South America monsoons</p> <p>Iracema Cavalcanti iracema.cavalcanti@cptec.inpe.br Dr. Cavalcanti is expert in climate change and extreme events in South America</p> <p>Anji Seth anji.seth@uconn.edu Dr. Seth is expert in regional modeling and climate variation and changes in South America and North America</p> <p>Prakki Satyamurty saty.prakki@gmail.com Dr. Satyamurty is expert in climate of South America, including extreme temperature</p> <p>Francisco Cruz University of Sao Paulo chico.bill@usp.br</p>

Dr. Cruz is expert in paleoclimate and climate change in monsoons regions.

July 29, 2012

Dear Editor of Journal of Climate

We would like to submit the manuscript entitled “**CMIP5 Simulations of Low-Level Tropospheric Temperature and Moisture over tropical Americas**”, by Leila M. V. Carvalho and Charles Jones as part of the special collection “North America in CMIP5 models”. The paper has 16 figures (8 color figures) and 2 tables. This paper discusses temperature and moisture trends in tropical Americas using two reanalyses and 11 CMIP5 simulations (for the 20th century run and the RCP8.5).

Thank you very much for your attention,

Dr. Leila M. V. Carvalho

Dept. Geography, University of California, Santa Barbara

Earth Research institute, University of California, Santa Barbara

leila@eri.ucsb.edu

Copyright Form

[Click here to download Copyright Form: copyright-leila.pdf](#)

Page and Color Charge Estimate Form

[Click here to download Page and Color Charge Estimate Form: page_charge_leila.pdf](#)

CMIP5 Simulations of Low-Level Tropospheric Temperature and Moisture over tropical Americas

Leila M. V. Carvalho ^{1, 2} and Charles Jones ²

¹ Department of Geography, University of California, Santa Barbara, CA, USA

² Earth Research Institute, University of California, Santa Barbara, CA, USA

Journal of Climate

Submitted: July 2012

Corresponding author address: Dr. Leila M. V. Carvalho, Dept. Geography, University of California Santa Barbara, CA 93106, USA.

Email: leila@eri.ucsb.edu

Abstract

Global warming has been linked to systematic changes in North and South Americas climates and may severely impact the North American and South American Monsoon systems (NAMS and SAMS, respectively). Monsoon characteristics (e.g, onset, duration and seasonal amplitude) depend greatly on the magnitude and spatial extent of the land-ocean temperature contrast and atmospheric moisture content, among other factors. This study examines interannual-to-decadal variations and changes in the low-troposphere (850hPa) temperature (T850) and specific humidity (Q850) over the NAMS and SAMS using NCEP/NCAR and CFSR reanalyses and fifth phase of the Coupled Model Intercomparison Project (CMIP5) simulations for two scenarios: “historical” and high emission representative concentration pathways “RCP8.5”. Trends in the magnitude and area of the 85th percentiles were distinctly examined over SAMS and NAMS regions during the peak of the respective monsoon seasons. The historical simulations (1951-2005) and the two reanalyses agree well and indicate that significant warming has occurred over tropical South America with a remarkable increase in the area and magnitude of the 85th percentile in the last decade (1996-2005). The RCP8.5 CMIP5 ensemble mean projects an increase in the T850 85th percentile of about 2.5°C (2.8°C) by 2050 and 4.8°C (5.5°C) over South America (North America) by 2095 relative to 1955. The area of South America (North America) with $T850 \geq$ the 85th percentile is projected to increase from ~10% (15%) in 1955 to ~58% (~33%) by 2050 and ~80% (~50%) by 2095. This progressive warming is associated with an increase in the 85th percentile of Q850 of about 3g kg⁻¹ over SAMS and NAMS by 2095.

1. Introduction

The presence of a monsoonal type of circulation involving intense convective activity and heavy precipitation is the dominant climatic feature in the tropical Americas during the respective summer seasons. The North American monsoon system (NAMS) and the South American monsoon system (SAMS) are often interpreted as the two extremes of the seasonal cycle of heat, moisture transport and precipitation over the Americas (Vera et al. 2006).

NAMS extends from the intertropical zone of the eastern Pacific Ocean to the Bermuda high and from Central America to Canada (Ropelewski et al. 2005; Mechoso et al. 2005). Rainfall associated with NAMS accounts for about 70% of the annual total precipitation over a large area centered in northwest Mexico (e.g., Douglas et al. 1993). In the United States, NAMS directly influences precipitation regimes in New Mexico and Arizona where more than 40% and 25% of annual precipitation, respectively, is received during summer (Douglas et al. 1993; Higgins et al. 1997, 1999; Adams and Comrie 1997). There are also lowland areas associated with NAMS: the lower Colorado River valley and neighboring low desert areas. These regions play a significant role in the formation of the thermal low, which is an important feature of NAMS (Adams and Comrie 1997). In the present climate, the onset of NAMS occurs between May-June, when precipitation intensifies along the western slopes of the Sierra Madre Occidental (Douglas et al. 1993; Adams and Comrie 1997). NAMS is fully developed from July-August to early September and its demise occurs during late September and early October (e.g., Vera et al. 2006).

Convection migrates from Central America into South America by September. The onset of the rainy season over the Amazon is preceded by an increase in the frequency of the northerly cross-equatorial flow over South America that increases moisture in the boundary layer

(Marengo et al. 2001; 2010; Wang and Fu 2002). The onset of the wet season in central and southeastern Brazil in the present climate typically occurs between September and October (Silva and Carvalho 2007; Gan et al. 2004; Raia and Cavalcanti 2008). SAMS peaks from December through February when the main convective activity is centered over central Brazil and linked to a northwest-southeast oriented band of cloudiness and precipitation that often extends over western subtropical Atlantic and is known as the South Atlantic convergence zone (Kodama 1992; Carvalho et al 2002). SAMS demise over central eastern Brazil typically occurs from March to mid April (e.g. Silva and Carvalho 2007; Marengo et al. 2010).

The SAMS and NAMS seasonal cycles are essentially driven by the differential heating between the continent and ocean. In the pre-monsoon season, the incoming solar radiation increases the diabatic heating over the tropical continent and land-ocean contrasts initiate the monsoonal circulations. The differential heating strengthens the cross equatorial moisture transport by the trade winds toward the continent. Thermodynamic instability increases as the onset of the rainy season approaches and remains large throughout the wet season (Fu et al. 1999; Fu and Li 2004, Fisch et al. 2004). Convective activity intensifies on broad ranges of spatial and temporal scales to redistribute the excess of moist static energy accumulated near the surface (Adams and Comrie 1997; Rickenbach et al. 2011). Land-atmosphere processes control evapotranspiration and play a significant role on the onset and maintenance of the SAMS (Fu and Li 2004) and NAMS (Gutzler and Preston 1997; Gutzler 2000).

The global mean concentration of carbon dioxide and associated atmospheric radiative forcing has dramatically increased in the last decades (Foster et al. 2007). Changes in atmospheric forcing modify the distribution of the atmospheric heating with consequences to the hydrological cycle. The atmospheric moisture content increases in response to global warming

following the Clausius-Clapeyron relationship, but the rate of precipitation increase is slower as predicted by climate models (Allen and Ingram 2002; Richter and Xie 2008; Cherchi et al. 2011). Model results and future scenarios of climate change indicate that rainfall tends to increase in convergence zones with large climatological precipitation and to decrease in regions with subsidence (Chou and Neelin 2004; Chou et al. 2009).

Cherchi et al (2011), for instance, performed a set of experiments with a state-of-the-art coupled general circulation model forced with increased atmospheric CO₂ concentration (2, 4, and 16 times the present-day mean value) and compared with a control experiment to evaluate the effect of increased CO₂ on the monsoons. They concluded that all monsoon areas experience an enormous increase of vertically integrated specific humidity when the atmospheric carbon dioxide concentration is increased in the climate simulations, in consonance with the Clausius-Clapeyron relationship. However, the precipitation rate increase is smaller than the moisture content rise (Allen and Ingram 2002). The dominant player in the precipitation changes obtained by comparing the sensitivity experiments with a control simulation is the so-called q-term (thermodynamic component), i.e., the term that depends on the water vapor content change. Vertical velocity changes, horizontal moisture advection and the evaporation play different roles depending on the region of the monsoon (Cherchi et al 2011). The authors found that NAMS and SAMS experience a precipitation increase in the sensitivity experiments relative to the control mostly driven by the intensification of the upward motion. Moreover, they showed that over South America, the moisture transport from the Atlantic Ocean is increased in all CO₂ experiments compared to the control.

Carvalho et al. (2012) used NCEP/NCAR reanalyses-1 (Kalnay et al. 1996) and a multivariate large-scale monsoon index based on low-level (850hPa) circulation, temperature

and specific humidity and several precipitation data sets and showed evidence that SAMS has intensified in the last decades. Interesting enough, the pattern of intensification is quite similar to the pattern of increased precipitation shown in the sensitivity experiments with increased CO₂ (Cherchi et al. 2011). In addition, Carvalho et al. (2012) showed that the intensification of SAMS is mostly observed south of 15°S whereas drier conditions have been observed over eastern Amazon in recent years. The authors have related the subtropical intensification of SAMS and drying over eastern Amazon to the patterns of warming and changes in land-ocean temperature contrasts, moisture transport and moisture convergence over tropical South America.

Motivated by these studies, Jones and Carvalho (2012) investigated two reanalyses and fifth phase of the Coupled Model Intercomparison Project (CMIP5) (Taylor et al. 2011) simulations for two scenarios (“historical” and high emission representative concentration pathways “RCP8.5”). They used the same large-scale monsoon index discussed in Carvalho et al. (2012). The two reanalyses and 10 CMIP5 model simulations (historical experiment) consistently show statistically significant increases in seasonal amplitudes, early onsets, late demises and durations of the SAMS and are associated with extensive warming and moistening over tropical South America. The results convincingly support the hypothesis that recent decadal changes in the SAMS are forced by anthropogenic and natural changes in atmospheric composition and likely modifications in land-cover and land-use in South America. Jones and Carvalho (2012) also analyzed future changes in the SAMS with six CMIP5 model simulations of the RCP8.5 high emission scenario. All simulations unquestionably show significant increases in seasonal amplitudes, early onsets and late demises of the SAMS. The simulations for this scenario project a 47% increase in the amplitude by 2045-2050. Conversely, Maloney et al. (2012) examined changes in December-February (DJF) and June-August (JJA) ensemble mean

precipitation from CMIP5 simulations for the RCP8.5 scenario. Their results project a decrease in JJA precipitation over the NAMS region during 2070-2099 relative to 1961-1990 with large anomalies over western Mexico.

Inspired by these previous studies and the availability of CMIP5 simulations, this work investigates changes in the lower troposphere (850hPa) temperature and specific humidity over the SAMS and NAMS domains. CMIP5 simulations for two scenarios are examined: historical high emission representative path way (RCP8.5). Although it is unquestionable that the radiative forcing of the RCP8.5 experiments will result in increased mean temperatures and specific humidity comparatively to the historical runs (Allen and Ingram 2002), assessing the patterns of warming and moistening, magnitude and rate of change is critical to evaluate projected climate changes in monsoon regions.

This paper specifically focuses on interannual-to-decadal variations and changes of the 85th percentiles of temperature and specific humidity at 850hPa over South America (SA) and North America (NA) during the peak of SAMS and NAMS (December-February and July-August, respectively). We demonstrate that the 85th percentiles are predominantly observed over continental tropical areas and their increase in magnitude and spatial extent are good indicators of the expansion of the warming and moistening over North America (NA) and South America (SA). These aspects are investigated with daily average reanalyses and CMIP5 model experiments (section 2). We first examine the consistency between the two reanalyses and 11 CMIP5 simulations for the historical runs over South America (section 3.1) and North America (section 3.2). We then investigate the RCP8.5 projections of the expansion of the warming and moistening over South America (section 3.3) and North America (section 3.4). Summary and conclusions are presented in section 4.

2. Data

The large-scale features of T850 and Q850 over the SAMS and NAMS regions were characterized with daily reanalysis from the National Centers for Environmental Prediction/National Center for Atmospheric Research at 2.5° lat/lon grid spacing and during 1 January 1948-31 December 2010 (hereafter NCEP/NCAR) (Kalnay et al. 1996; Kistler et al. 2001). In addition, daily Climate Forecast System Reanalysis (CFSR) (Saha et al. 2010) was used at 0.5° lat/lon grid spacing during 1 January 1979-31 December 2010. The advantages of CFSR relative to NCEP include high horizontal and vertical resolutions, improvements in data assimilation and first-guess fields originated from a coupled atmosphere-land-ocean-ice system (Higgins et al. 2010; Saha et al. 2010). This study analyzes daily averages of specific humidity (Q850) and temperature (T850) at 850-hPa. These variables are important to characterize the onset, duration and amplitude of SAMS (Silva and Carvalho, 2007; Carvalho et al. 2011a,b; Carvalho et al. 2012; Jones and Carvalho 2012).

Changes in the above variables were examined with multi-model simulations from the fifth phase of the Coupled Model Intercomparison Project (CMIP5) (Taylor et al. 2011). CMIP5 model simulations provide the basis for the Fifth Assessment Report (AR5) of the Intergovernmental Panel on Climate Change (IPCC). Additional information about CMIP5 can be found at <http://cmip-pcmdi.llnl.gov/cmip5/>.

The following model experiments were examined. The “*historical*” run (also known as “20th century simulation”) was forced by observed atmospheric composition changes which include both anthropogenic and natural sources as well as time-evolving land cover. The historical run covers the period 1 January 1951 to 31 December 2005. In addition, CMIP5

simulations of climate projection are forced with specified concentrations referred to as “representative concentration pathways” (RCPs) and provide a rough estimate of the radiative forcing in the year 2100 relative to pre-industrial conditions (Moss et al. 2010; Taylor et al. 2011). To investigate future changes in the SAMS and NAMS, the “high-emission” scenario labeled as “RCP8.5” was used. In this scenario, radiative forcing increases throughout the twenty-first century before reaching a level of $\sim 8.5 \text{ W m}^{-2}$ at the end of the century. RCP8.5 simulations cover the period 1 January 2006-31 December 2100. The focus of the analysis is during the peak of the SAMS (December-February) and NAMS (June-August).

Table 1 alphabetically lists the models used in this study. The analysis of the historical experiments includes all 11 models. Due to difficulties in accessing CMIP5 data and to examine future projections in which the daily historical and RCP8.5 simulations were available with the same resolution, the following models were analyzed for the RCP8.5 scenario: CanESM2, GFDL-ESM2M, MPI-ESM-LR, MRI-CGCM3 and NorESM1-M. In addition, given the large volume of data, only one run from each model and experiment was used in this study. Although more models are currently available in CMIP5, at the time this work was conducted, daily outputs were available only for the models listed in Table 1.

3. Changes in T850 and Q850 over tropical Americas.

The primary focus of this study is on the SAMS and NAMS region. Uncertainties in precipitation regimes and unrealistic features in the tropical Americas in the CMIP3 simulations have been largely documented (e.g. Bombardi and Carvalho 2009; Vera and Silvestri 2009; Seth et al. 2010). Similar problems still persist in CMIP5 model simulations (Jones and Carvalho 2012; Shiffeld et al 2012). On the other hand, precipitation and cloudiness are related to low-

181 troposphere temperatures and humidity (e.g, Cherchi et al 2011). In order to assess and compare
182 CMIP5 projections of T850 and Q850, we focused our analysis on the 85th percentiles during the
183 peak of the NA and SA monsoon seasons (that is, JJA and DJF respectively). This method is
184 useful because it does not make any pre-assumptions about the geographic location of the
185 monsoons that may vary among the CMIP5 simulations. The 85th percentiles of T850 and Q850
186 (henceforth referred to as T850_{p85} and Q850_{p85}, respectively) were calculated separately over
187 North America during JJA and over South America during DJF. Only grid points with elevation
188 below 1500m were used in the calculation. For simplicity, Central America was included in the
189 calculation of percentiles over the North America domain. As we will show in the following
190 discussions, T850_{p85} and Q850_{p85} extends over tropical continental areas and are strongly linked
191 to the American monsoon regions in the reanalyses and historical runs.

192 Two main aspects were investigated in these analyses: the area extent of the 85th
193 percentiles and the interannual variation in the magnitude of the percentiles. The following
194 approaches were adopted. The 85th percentiles were calculated for CMIP5 historic runs and for
195 NCEP/NCAR reanalysis considering all DJF (JJA) seasons from 1951 to 2005 for South
196 America (North America) (Table-2). Similar procedure was adopted for CFSR reanalysis except
197 that the range of years extended from 1979-2005. Changes in the area of the 85th percentiles in
198 the historical and RCP8.5 simulations and in the NCEP/NCAR and CFSR reanalyses were
199 calculated using the values of the 85th percentiles obtained for the 20th century run. The main
200 purposes of using fixed values of the 85th percentile for NA and SA were to examine patterns of
201 warming and moistening of the low troposphere, identify areas with rapid changes and assess
202 uncertainties in the CMIP5 models by comparing them with the two reanalyses.

The magnitudes of the 85th percentile were calculated for each DJF (JJA) season over South America (North America) and for the historical and RCP8.5 runs. All CMIP5 models show unrealistic large variance on interannual times-scales in the variables T850 and Q850 (not shown). Thus, to investigate long-term changes in these variables, all data in the historical and RCP8.5 runs were smoothed with a 9-year moving average.

CMIP5 simulations exhibit significant biases in T850 in NA and SA. CanESM2, CSIRO-Mk3.6 and MIROC4H are systematically warmer than CFSR and NCEP/NCAR reanalyses and warmer than all other models. CanESM2 exhibits the largest positive bias in T850 followed by CSIRO-Mk3.6 and MIROC4H over NA and SA. On the other hand, INM-CM4 shows the largest T850 negative biases over tropical Americas. By comparing the 85th percentiles (Table-2), it is noticeable that with exception of CanESM2, CSIRO-Mk3.6, MIROC4H and HadCM3, all other models show differences in T850_{p85} of less than 1°C (or less than 5%) over tropical SA when compared to NCEP/NCAR reanalysis during the same period. On the other hand, differences are larger for T850_{p85} over NA, with GFDL-ESM2M and MRI-CGCM3 exhibiting the largest negative differences relatively to NCEP/NCAR.

CMIP5 historical simulations also exhibit biases in Q850. Table-2 shows that the largest differences relative to NCEP/NCAR are observed for MRI-CGCM3 over SA (+1.05g/kg or ~9%). CSIRO-Mk3.6 overestimates T850_{p85} over SA and NA. MRI-CGCM3 shows positive differences of about 9% in the Q850 85th percentile over SA but about 4% over NA. IPSCM5-ALR shows the largest negative differences in Q850_{p85} for SA (~7.49%) and NA (~13.5%).

3.1 Historical Runs: South America

Decadal variations in the area with T850 greater or equal T850_{p85} in the historical runs and in the two reanalyses during DJF are shown in Fig. 1. The NCEP reanalysis (Fig. 1a) indicates a progressive warming over central-eastern South America since 1956. Similar pattern of variability in T850 has been identified in Carvalho et al. (2012) from SAMS onset to demise. CFSR reanalysis (Fig. 1b) shows similar pattern, with the most remarkable differences occurring in the last decade (1996-2005) comparatively with the previous ones. It is noticeable that the 85th percentile is larger for CFSR than NCEP/NCAR, which partially explains the differences in the spatial patterns. In addition, the period (1979-1985) is shorter than the equivalent period (1976-1985), which contributes to the observed differences. Notice that the largest warming has occurred where SAMS exhibits its largest seasonal variability (e.g. Silva and Carvalho 2007; Carvalho et al. 2011a,b, Raia and Cavalcanti 2008, Gan et al. 2004).

The majority of the CMIP5 models simulate well the pattern of warming over tropical SA, in particular the remarkable expansion of T850_{p85} in the 1996-2005 decade (Fig. 1c-m). The eastward enlargement of the T850_{p85} over central-eastern South America in the 1996-2005 decade comparatively with the 1956-1965 decade is evident in most models, with exception of CanESM2 (Fig. 1k) and CSIRO-Mk3.6.0 (Fig. 1l) that show a signal of the recent warming over northwestern Amazon. Regional differences in the spatial pattern of the warming are in some way related to the large degree of uncertainty in the simulations of cloudiness and precipitation in the tropical regions that have been documented previously in analyses of CMIP3 (Bombardi and Carvalho 2009, Silvestre and Vera 2009) and CMIP5 historical runs (Jones and Carvalho 2012; Sheffield et al. 2012). Some models such as the MPI-ESM-LR (Fig. 1e), IPSL-CM5A-LR (Fig. 1h), HadCM3 (Fig. 1j), CNRM-CM5 (Fig. 1m) CanESM2 (Fig. 1k) and CSIRO-Mk3.6.0 (Fig. 1l) indicate temperatures above T850_{p85} over the western Amazon that do not seem realistic

when compared to the two reanalyses. It is worth noting that GFDL-ESM2M (Fig.1c) T850_{p85} pattern of warming is quite consistent with the CFSR reanalysis (Fig. 1b) over eastern SA especially in the last decade of the historical simulation.

The interannual variation of T850_{p85} (9-year moving average) in the CMIP5 historical simulations and CFSR and NCEP/NCAR reanalyses are shown in Fig. 2a. The NCEP/NCAR reanalysis shows a cold bias and more moderate warming trend comparatively to CFSR. The NCEP/NCAR slope of the linear trend over the 1955-2000 period is about 0.024°C yr⁻¹ whereas the respective slope for the CFSR reanalysis is about 0.03°Cyr⁻¹ (1983-2000). All models underestimate the NCEP/NCAR trend with exception of GFDL-ESM2M and CanESM2 (0.02°Cyr⁻¹ and 0.025°Cyr⁻¹, respectively). To assess the performance of the CMIP5 models in simulating the observed trends in T850_{p85} regardless existing biases in T850, the intercept of the linear fit of all CMIP5 model simulations was removed and the resulting temperature anomalies (plus trends) are displayed in Fig. 2b. The intercepts do not differ significantly from the mean values over the historical period for NCEP/NCAR and CMIP5 models. Nonetheless, since all CMIP5 models and the two reanalyses exhibited linear trends during the historical period, the intercepts were removed to allow a comparison with short record of CFSR. The resulting CMIP5 ensemble mean, minimum and maximum anomalies are plotted along with NCEP/NCAR and CFSR anomalies. Figure 2b reinforces that the observed magnitude of the temperature anomalies were well captured by the maximum CMIP5 anomalies (dominated by GFDL-ESM2M and CanESM2). Trends that result from the ensemble mean are not realistic for SA. For instance, NCEP/NCAR shows an increase of 1.0°C in the 85th percentile from 1955-2000. CFSR reanalysis indicates that the NCEP/NCAR reanalysis may have underestimated temperature

anomalies in about 0.5°C. The CMIP5 ensemble mean indicates much less increase in temperature (about 0.5°C) between 1955 and 2000.

Figure 2c examines the interannual variation in the area with $T850 \geq T850_{p85}$ over SA. We recall that the areas were obtained for $T850_{p85}$ calculated over the entire 1951-2005 period. The area was calculated for each DJF season and further smoothed with a 9-year moving average. Given the differences in resolution among models and reanalyses and implications for the estimation of the area, Fig. 2c shows the fraction (percentage) of SA that was observed with $T850 \geq T850_{p85}$. There is good agreement among CMIP5 models and NCEP/NCAR reanalysis, with all models showing positive trends. In addition, most models show an increase in the slope of the positive trend in the last two decades, as suggested in Fig. 1. CFSR indicates a large trend (0.70% yr⁻¹) during 1979-2000. NCEP/NCAR reanalysis indicates a weaker trend (0.45% yr⁻¹) during 1955-2000. It is worth noticing that trends increase around 1993 in both reanalyses.

Decadal variations in $Q850_{p85}$ for the historical simulations are investigated in Figs 3-4. Figures 3(a,b) indicate that CFSR and NCEP/NCAR exhibit distinct patterns of decadal variations of $Q850_{p85}$. NCEP/NCAR shows $Q850_{p85}$ displaced towards northwestern Amazon, whereas CFSR shows a much broader area extending from Central Amazon toward southeastern Brazil resembling the South Atlantic Convergence Zone (Carvalho et al. 2002). In addition, CFSR shows a remarkable increase in $Q850_{p85}$ in the 1995-2005 decade. These features are quite consistent with trends in SAMS (Carvalho et al. 2012; Jones and Carvalho 2012) and to some extent to trends in extreme precipitation over southeastern Brazil (Silva Dias et al. 2012, Cavalcanti 2012). Dessler and Davis (2010) argue that the NCEP/NCAR reanalysis-1 (used in this study) contains large biases in specific humidity in the tropical mid and upper troposphere

which could explain the differences with respect to the more comprehensive data assimilation used in the CFSR reanalysis.

Although the spatial patterns of $Q850_{p85}$ do not necessarily coincide with the patterns of $T850_{p85}$, most CMIP5 models show progressive increases in $Q850_{p85}$ over the SAMS region, more evident in the last 1-2 decades of the historic runs, which is consistent with the warming of the low-troposphere (Cherchi et al. 2011). INMC is the most conservative model, showing an increase in $Q850_{p85}$ only in the last decade and over eastern Brazil. IPSL-CM5A-LR (Fig. 3h) is the only model that indicates a decrease in $Q850_{p85}$ over southeastern Brazil from the first (1956-1965) to the last decade (1996-2005). Nonetheless, the CMIP5 models most consistent feature is the decadal increase in $Q850_{p85}$ over the Amazon basin, which is supported by CFSR (Fig. 3b).

Figure 4a shows interannual variations of the 9-yr moving average of $Q850_{p85}$. NCEP/NCAR shows a negative bias with respect to CFSR as suggested in Dessler and Davis (2010). Nonetheless, both reanalyses show positive trends in $Q850_{p85}$, consistent with the warming of the lower troposphere. NCEP/NCAR indicates a linear trend of $\sim 0.008 \text{ g kg}^{-1} \text{ yr}^{-1}$ (1955-2000). The NCEP/NCAR trend in $Q850_{p85}$ is not constant. The CFSR trend is $\sim 0.016 \text{ g kg}^{-1} \text{ yr}^{-1}$ (1983-2000) whereas the NCEP/NCAR trend is $\sim 0.010 \text{ g kg}^{-1} \text{ yr}^{-1}$ in the same period (1983-2000). All CMIP5 models indicate positive trends in $Q850_{p85}$ varying from $0.005 \text{ g kg}^{-1} \text{ yr}^{-1}$ (MRI-CGCM3) to $0.014 \text{ g kg}^{-1} \text{ yr}^{-1}$ (MPI-ESM-LR). However, MPI-ESM-LR shows the largest positive bias in $Q850_{p85}$. Figure 4b exhibits the historical CMIP5 ensemble mean, maximum and minimum $Q850_{p85}$ along with NCEP/NCAR and CFSR reanalyses. The CMIP5 ensemble mean is remarkably consistent with CFSR.

The CMIP5 ensemble mean, maximum and minimum of the fraction of SA with $Q850 \geq Q850_{p85}$ are shown in Fig 4c. In spite of differences in the spatial patterns of $Q850_{p85}$, NCEP/NCAR is within the range of variation of the CMIP5 models. There is a large discrepancy between CFSR and NCEP/NCAR, which is also evident in the decadal variation of $Q850_{p85}$ (Fig. 3b). CFSR exhibits a sharp change in the slope around 1993 that can be also identified in $T850_{p85}$ (Fig. 2c). All CMIP5 models show large areal coverage of $Q850 \geq Q850_{p85}$ when compared to CFSR.

3.2: Historical Runs: North America

Decadal variations in the area with $T850 \geq T850_{p85}$ in the CMIP5 historical runs and in the two reanalyses during JJA are shown in Figs. 5-6. $T850_{p85}$ largely extends over the area dominated by NAMS (e.g. Barlow et al. 1998) in the two reanalyses and in all CMIP5 simulations (Fig. 5). We emphasize that due to the coarse resolution of the models and steep topography, these analyses underrepresent existing variations and changes in many valleys located in the NAMS domain. Nonetheless, NCEP/NCAR (Fig. 5a) and CFSR (Fig. 5b) indicate a modest increase in the area with $T850_{p85}$ over NA during 1996-2005 comparatively to previous decades with progressive warming southeastward of the U. S. Most CMIP5 models show similar trends, with exception of NorESM1-M that shows almost no changes over the U.S. in the historical run (Fig. 5f). Moreover, it is worth noting that all models indicate an increase in temperature off the coast of Baja California toward the eastern Pacific. Opposite trends are shown in the NCEP/NCAR reanalysis (Fig. 5a). The eastern Pacific stratocumulus clouds (Yuter et al. 1997) are likely among the causes of the uncertainties in the simulations of the CMIP5 in the region (Bony and Dufresne, 2005).

Figure 6a shows the NCEP/NCAR, CFSR and CMIP5 interannual variations of $T850_{p85}$ (9-yr moving average) calculated over NA. CFSR correlates well with NCEP/NCAR (linear correlation of about 0.96) but shows $T850_{p85}$, on average, 0.33°C warmer than NCEP/NCAR, with differences increasing up to 0.5°C in the last decade. CanESM2, CSIRO-Mk3.6.0, CNRM-CM5 and MIROC4H overestimate both reanalyses, with mean biases ranging from 1.0°C (MIROC4H) to 3.4°C (CanESM2) relative to the NCEP/NCAR mean. All other CMIP5 models underestimate NCEP/NCAR (and therefore CFSR); MRI-CGCM3 shows the largest negative bias (-2.19°C) and HadCM3 the least bias among all CMIP5 models investigated here (-0.15°C). With exception of CNRM that shows no trend in the historical run, all other models indicate a positive trend in $T850_{p85}$, with rates that increase at the end of the historical period. Figure 6b shows the CMIP-5 ensemble mean, maximum and minimum temperature anomalies (plus linear trends) and reanalyses after removing the intercept of the linear fit. As stated before, this was done to remove the bias in the models and compare CMIP5 with the reanalyses. Figure 6b indicates that the CMIP5 ensemble mean shows good agreement in simulating the observed trend in the anomalies in recent decades as indicated by CFSR and NCEP/NCAR reanalyses. The NCEP/NCAR and CFSR are within the minimum and maximum ranges of the CMIP5 $T850_{p85}$ anomalies.

Figure 6c shows interannual variations of the fraction of NA with $T850 \geq T850_{p85}$. NCEP/NCAR does not indicate any linear long-term trend in area during the 1955-2001 period. A method for detection of shifts in the mean (Rodionov 2004) (using a sliding window of 10 years and 5% significance level) was applied to NCEP/NCAR time series and indicated that changes in the regime of the mean occurred in 1962, 1977 and 1996. Moreover, the consistency between NCEP/NCAR and CFSR is also noticeable. CMIP5 ensemble mean, maximum and

minimum indicate a progressive increase in the area with $T850 \geq T850_{p85}$ and an increase in the slope of the trend from 1985-2001 (Fig. 6c).

The decadal variation of areas with $Q850_{p85}$ for NA in JJA is shown in Fig. 7. NCEP/NCAR (Fig. 7a) indicates a progressive increase of the 85th percentile over NA and eastern Pacific, north of the Equator. Over NA, the largest increase in area is observed over central and southern U. S., east of the Rockies. On the other hand, CFSR (Fig. 7b), seems consistent over eastern Pacific north of the equator, but indicates a negative trend over south and southeast U.S. This region has been affected by long-term droughts (Samanta et al. 2011) and CFSR has an improved data assimilation and higher resolution to identify these regional patterns. All CMIP5 models show an expansion of areas with $Q850_{p85}$ over the NAMS domain and Florida (Fig. 7c-l). The CMIP5 patterns of decadal variability of $Q850_{p85}$ over NAMS are quite consistent with NCEP/NCAR.

Figure 8a shows the CMIP5 interannual variations of $Q850_{p85}$ over NA in JJA along with the two reanalyses. CFSR and NCEP/NCAR differ in magnitude and interannual variability. CFSR 85th percentile is about 0.5 g/kg greater than NCEP/NCAR. CFSR shows a decrease in the 9-yr moving average of $Q850_{p85}$ after 1996, while NCEP/NCAR shows a positive trend during the same period. CSIRO-Mk3.6.0 has the largest positive bias (>1g/kg) whereas IPSL-CM5A-LR has the largest negative bias (<1.g/kg) with respect to the two reanalyses. Interesting enough, MIROC4H, CanESM2 show ranges of magnitudes that are similar to NCEP/NCAR, in spite of the relatively large positive biases in $T850_{p85}$ (Fig. 6a). The resulting CMIP5 ensemble mean, maximum and minimum $Q850_{p85}$ along with the two reanalyses are shown in Fig. 8b. The CMIP5 ensemble mean agrees quite well with NCEP/NCAR, but underestimates CFSR. The fraction of NA with $Q850 \geq Q850_{p85}$ in JJA is shown in Fig. 8c. The CMIP5 ensemble mean is

consistent with NCEP/NCAR after 1979 and indicates an increase of about 2% in the area with $Q850 \geq Q850_{p85}$ from 1955-2001. CFSR shows a decrease in $Q850_{p85}$ that is not identified by NCEP/NCAR. It is worth noticing that the decrease in the extent of the moist regions over NA identified with CFSR does not reflect the trend in $T850_{p85}$ (Figs. 6a,c)

3.3 RCP8.5 Future Projections: South America.

Figure 9 shows CMIP5 projections of decadal variations of $T850_{p85}$ for SA in DJF during 2006-2095. We recall that the projections use the same thresholds obtained for the historical runs. All models project a continued expansion of $T850_{p85}$ toward eastern tropical SA and the Equatorial Atlantic and Pacific. These trends follow the patterns of warming that have been observed in the historical runs and for NCEP/NCAR and CFSR reanalyses (Fig. 1). Notice that no CMIP5 model projects the extension in area of $T850_{p85}$ south of 40°S over SA and south of 30°S over the South Atlantic. The spatial patterns of the trends suggest a decrease in temperature gradients near the equator and an increase in subtropical latitudes. These projections, if confirmed, will critically impact SAMS characteristics by modifying ocean-land temperature contrasts and low-level moisture convergence.

Figure 10a shows the projections of the anomalies using the same methodology discussed in Fig. 2a. NCEP/NCAR and CFSR 9-year moving averages have been extended until 2005. The ensemble mean is consistent with NCEP/NCAR whereas the ensemble maximum seems to be closer to CFSR. The ensemble mean projects that $T850_{p85}$ will be 2.5°C (4.7°C) above the values observed in 1955 by 2050 (2095). Considering that the maximum projected anomalies are more consistent with CFSR, one might expect $T850_{p85}$ anomalies of about 4.5°C over SA by 2050 under the RCP8.5 scenario.

The expansion in area of the $T850_{p85}$ calculated for the historical runs are shown in Fig. 10b. The ensemble mean is very consistent with both reanalyses, particularly in recent decades, suggesting high confidence in the projected trends. CMIP5-ensemble mean, CFSR and NCEP/NCAR indicate that the $T850_{p85}$ extend over an area that represents approximately between 25% and 30% of SA. By 2050 this area might double (i.e., reach 60% of SA) according to the CMIP5 RCP8.5 ensemble mean projections. This trend would continue until the end of the century when it would reach ~80% of the continent, extending largely over tropical SA and likely affecting SAMS characteristics.

Projections of decadal variations in $Q850_{p85}$ are displayed in Fig. 11. As shown for the historical runs, all CMIP5 models indicate an increase in $Q850$ over the tropics in agreement with the patterns of warming in the lower troposphere shown in Figs 10. The expansion of areas with $Q850 \geq Q850_{p85}$ over the Amazon basin has been confirmed by averaging CFSR in recent years (2006- 2010 – not shown). During this period, CFSR shows that $Q850_{p85}$ has largely expanded over the Amazon Basin and southeastern Brazil, supporting the CMIP5 projected trends in $Q850_{p85}$.

Figure 12a summarizes the projected CMIP5 ensemble mean of $Q850_{p85}$ over SA. In spite of differences in spatial patterns, there is an extraordinary agreement between the ensemble mean and CFSR. The ensemble mean suggests that $Q850_{p85}$ would increase 1g/kg from the present value (~12.4g/kg) by 2050 and ~ 3.0g/kg by 2095. The fraction of SA with $Q850_{p85}$ would increase from approximately 30% in the 2000-2010 decade to about 58% around 2050. This fraction might increase to about 70% in 2095.

3.4 RCP8.5 Future Projections: North America.

CMIP5 projections of decadal variations in $T850_{p85}$ over NA in JJA are examined in Fig. 13. All CMIP5 models project progressive increases in the area with $T850 \geq T850_{p85}$ that extends beyond NA, including tropical SA. These are remarkable findings, given that it is winter in SA and the 85th percentile for NA is higher than the respective percentiles in SA during summer (see Table-2). Notice that only GFDL shows areas with temperatures greater or equal than $T850_{p85}$ calculated for NA over SA during JJA in the historical run (Fig. 5c). Another significant feature is the progressive expansion of the warming toward eastern U.S. and high latitudes, suggesting the expansion of tropical temperatures toward the extratropics of NA. The resulting changes in temperature gradients are consistent with the projected changes in the baroclinicity and resulting increase in precipitation over the extratropics of NA shown in Maloney et al. (2012)

Figure 14a shows future projections of $T850_{p85}$ anomalies over NA in JJA. To compare the historic with the RCP8.5 simulations, the CMIP5 ensemble mean, maximum and minimum were obtained after removing the intercept of the linear trends fitted for the historic run (Fig. 6a). It can be noticed that the CMIP5 minimum values seem consistent with NCEP/NCAR, whereas the maximum values follow CFSR. The ensemble mean projects an increase of $\sim 2.8^{\circ}\text{C}$ (5.5°C) from 1955-2050 (1955-2095). Projections of changes in the fraction of NA with $T850 \geq T850_{p85}$ in JJA are shown in Fig. 14b. There is a remarkable agreement among the reanalyses and the ensemble mean. The ensemble mean indicates that the warming could expand approximately 15% by 2050 and would reach 50% of NA by the end of the century. Most of this expansion would take place in the low troposphere of the U.S..

Projections of decadal changes in $Q850_{p85}$ are shown in Fig. 15. The most consistent projection among models is the progressive expansion of $Q850_{p85}$ from the tropics towards higher latitudes over central-eastern USA. Changes are much less pronounced in the West coast

of the USA. MRI-CGCM3 (Fig. 15b), MPI-ESM-LR (Fig. 15c), NorESM1-M (Fig. 15d) and CanESM2 (Fig. 15e) shows an expansion of $Q850_{p85}$ over eastern North Atlantic, suggesting the intensification of the warming in this region that is not necessarily identified from decadal changes in $T850_{p85}$ (compare Fig. 15 with Fig. 13)

Interannual variations and changes in the magnitude of $Q850_{p85}$ over NA in JJA are shown in Fig. 16a. As discussed before, there is good agreement between the ensemble mean and NCEP/NCAR. CFSR varies more consistently with the CMIP5 maximum projections. The ensemble mean indicates that $Q850_{p85}$ would increase from $\sim 10\text{g/kg}$ by 2006 to $\sim 11\text{g/kg}$ (12.5g/kg) by 2050 (2095). The ensemble mean projections of expansion in the fraction of NA with $Q850 \geq Q850_{p85}$ (Fig. 16b) suggest an increase in 15% of the area by 2050 and 50% by 2095.

4. Conclusions

This study examines the warming and moistening of tropical SA and NA with emphasis in the SAMS and NAMS domains. SAMS and NAMS significantly affect populated areas, ecosystems, water and energy management, agriculture, and food security for millions of people. The focus of this analysis is on the interannual to decadal variations and changes of the 85th percentiles of temperature and specific humidity in 850hPa. Temperature and moisture at 850hPa are less affected by land use and change and are yet related to the seasonal variations in the monsoon regimes. The 85th percentiles were calculated separately for NA and SA during the respective peaks of the summer seasons. It is shown that these percentiles extend where SAMS and NAMS show maximum seasonal variations in the climate of the 20th century (e.g. Vera et al. 2006).

This study investigates 11 CMIP5 model simulations of the ‘historical’ run and 6 models for the RCP8.5 projections. Two reanalyses are examined: NCEP/NCAR (1951-2010) and CFSR (1979-2010). These two reanalyses differ in resolution and data assimilation. It is shown that CFSR has a positive bias in temperature and moisture with respect to NCEP/NCAR. The short length of CFSR reanalysis in recent decades resulted in higher overall 85th percentiles and these percentiles were used to calculate decadal variations in the warming and moistening over NA and SA. However, the differences in the period of the reanalyses did not influence the calculation of the interannual variation of the 85th percentiles. In spite of existing biases in T850, the two reanalyses are well correlated over time. Large differences are observed in spatial and temporal patterns of Q850 and these differences may have largely resulted from differences in data assimilation schemes.

Two main aspects are investigated in this article: decadal variations and change of the warming and moistening of the lower troposphere over the tropics (identified with the 85th percentile of T850 and Q850, respectively) and interannual variations of the magnitudes and area extent of the percentiles. These features are examined separately for NA and SA during the respective peak of the monsoon season (JJA and DJF, respectively).

NCEP/NCAR and CFSR show progressive increases in the area with T850_{p85} over SA, with a remarkable extension over eastern Brazil, where SAMS exhibits its most significant seasonal variability (Marengo et al. 2010). All CMIP5 simulations of the historic run show similar increases in T850_{p85} over SA, and are particularly more consistent among themselves and with the two reanalyses in the last 1-2 decades. The CMIP5 ensemble mean underestimates the observed anomalies in T850_{p85} over SA. The maximum simulated anomalies seem to better represent the magnitude of the warming estimated with NCEP/NCAR and CFSR in the present

climate. The CMIP5 ensemble mean, maximum and minimum of the fraction of $SA \geq T850_{p85}$ is in the expected range of variations indicated by the two reanalyses. The trends in the ensemble mean are consistent with the trends of the two reanalyses, particularly in the last decade.

The RCP8.5 CMIP5 projections of $T850_{p85}$ over SA indicate that the warming over Eastern tropical SA would intensify and continuously expand over tropical eastern SA potentially affecting SAMS in the next decades. CMIP5 RCP8.5 simulations indicate that the maximum projected anomalies are more realistic when compared to CFSR, whereas the ensemble mean represents NCEP/NCAR quite well. The maximum projected anomaly for the RCP8.5 scenario indicates an increase in $T850_{p85}$ of about 4°C by 2050 and about 8°C by 2095 with respect to the beginning of the historical simulation. If one considers the ensemble mean projection, which is more consistent with NCEP/NCAR, the anomalies would be about 2.5°C by 2050 and 4.8°C by 2095. Less uncertainty is observed for the area with $T850 \geq T850_{p85}$ for SA when comparing the CMIP5 ensemble mean with the two reanalysis. The RCP8.5 scenario projects that about 60% of the area of SA would experience $T850 \geq T850_{p85}$ by 2050, which is double of the present area and 6 times larger than the area observed in the beginning of the historical period. The expansion in area is largely concentrated in the tropics and north of 30°S . These changes may affect land-ocean gradients with further implications to the characteristics of SAMS.

Large discrepancies are observed in the patterns of $Q850_{p85}$ over SA in the two reanalyses. NCEP/NCAR and CFSR show distinct patterns of decadal variations and changes in $Q850_{p85}$ over the tropics. CFSR shows $Q850_{p85}$ extending over the monsoon region in a spatial pattern that resembles the SACZ, whereas NCEP/NCAR shows that the 85th percentile is essentially observed over Northern Amazon. The NCEP/NCAR spatial features likely result from

problems in data assimilation and may not represent the actual pattern of Q850 over SA. CFSR shows a large increase in $Q850_{p85}$ over the Amazon basin in recent decades. Similar increase is also simulated by most CMIP5 models in the historical run. There is remarkable good agreement between the interannual variation of $Q850_{p85}$ from the CMIP5 ensemble mean and CFSR, which is of great value for future projections of climate change. The CMIP5 models overestimate the area with $Q850_{p85}$ based on CFSR. However, the trend in area in the last two decades is well simulated by the CMIP5 models.

The NCEP/NCAR and CFSR reanalyses do not show large decadal increases in the area with $T850_{p85}$ over the NAMS region. Most CMIP5 models are consistent with these observations and some show modest warming over central western USA during JJA. However, comparisons among the reanalyses and the CMIP5 historical simulations of the interannual variation of the magnitudes of the $T850_{p85}$ indicate large uncertainty, with the maximum anomalies more consistent with CFSR and minimum anomalies consistent with NCEP/NCAR. The ensemble mean captures well the overall trend of $T850_{p85}$ over NAMS, in particular the trends in the last three decades of the historical period. Furthermore, there is very good agreement between CFSR, NCEP/NCAR and the CMIP5 ensemble mean of the interannual variability of the area of NA with $T850 \geq T850_{p85}$. Although the positive trends in area and in the magnitude of $T850_{p85}$ are much less pronounced in the NAMS domain comparatively with the SAMS domain, the RCP85 scenario indicates that changes between 1-4°C in the magnitude may likely occur by 2050. The large anomalies are more consistent with CFSR in the CMIP5 historical simulations. We recall that due to the coarse resolution of most CMIP5 models and also the reanalyses (in particular NCEP/NCAR) there is an underrepresentation of the contribution of valleys and other areas located in complex terrain to the warming of the NAMS region. Nonetheless, the RCP85

simulations show remarkable and consistent expansions of the warm areas eastward of the present domain. Given the large extent of NA toward the extratropics, all models indicate that the $T850_{p85}$ (as calculated for the historical runs) would expand to mid-latitudes of NA. The CMIP5 RCP8.5 ensemble mean projects that the fraction of NA with $T850 \geq T850_{p85}$ would increase from about 15% in 2001 to approximately 35% by 2050 and will reach about 50% by 2095. These changes could largely affect the subtropics and extratropics of the U. S.

As observed for SA, there is a large discrepancy in $Q850_{p85}$ between the two reanalyses over NA. These differences seem to be particularly relevant over southern U. S. The CMIP5 ensemble mean shows interannual variations that are more consistent with NCEP/NCAR reanalysis, whereas CFSR is more consistent with CMIP5 maximum values. These discrepancies increase the uncertainties in the RCP8.5 projections of $Q850_{p85}$ area and magnitude. Nevertheless, the RCP8.5 CMIP5 ensemble mean projects an increase of about 1g/kg in $Q850_{p85}$ by 2050 and 2.5g/kg by 2095. These changes would be more relevant over large areas of the U. S., following the positive trend in temperature in these regions. More moisture in the lower troposphere would be observed also in the extratropics and may play a role for summer and winter storms in these regions, as suggested in Maloney et al. (2012).

Although future emissions and the adequate atmospheric radiative forcing to represent future scenarios of climate change are still debatable, the historical runs and reanalyses examined in this study have provided consistent evidence that critical changes in the climate over the tropical Americas, and in particular over the SAMS domain, have already occurred. Analyses similar to the ones discussed here were carried out for the CMIP5 pre-industrial experiment (labeled as “*picontrol*”) (not shown). The *picontrol* experiment prescribed pre-industrial atmospheric CO_2 concentrations and unperturbed land use. They provided additional evidence

that the expansion of the warming over tropical SA and trends in area and magnitude of the 85th percentiles observed in the historical runs and reanalyses are not spurious and are of anthropogenic origin.

Acknowledgements: The authors acknowledge the support of NOAA Climate Program Office Modeling, Analysis, Predictions and Projections (MAPP) Program as part of the CMIP5 Task Force. Work was supported under grant NA10OAR4310170. Authors acknowledge the support of the National Science Foundation RAPID program (grant AGS-1126804) and USAID-CIP (Sub-Contract SB100085). NCEP/NCAR Reanalysis was provided by the NOAA/OAR/ESRL PSD, Boulder, Colorado, USA (www.esrl.noaa.gov). CFSR reanalysis for this study are from the Research Data Archive (RDA) maintained by the Computational and Information Systems Laboratory (CISL) at the National Center for Atmospheric Research (NCAR). NCAR is sponsored by the National Science Foundation (NSF). We acknowledge the World Climate Research Programme Working Group on Coupled Modeling, which is responsible for CMIP, and we thank the climate modeling groups (listed in Table 1 of this paper) for producing and making available their model output. For CMIP, the U.S. Department of Energy's Program for Climate Model Diagnosis and Intercomparison provides coordinating support and led development of software infrastructure in partnership with the Global Organization for Earth System Science Portals.

REFERENCES:

Adams, D. K. and A. C. Comrie: The North American Monsoon. *Bull. Am. Meteor. Soc.* **78**, 2197-2213.

583 Allen, M.R., and W. J. Ingram, 2002: Constraints on future changes in climate and the
584 hydrologic cycle. *Nature*, **419**, 224–232.

585 Barlow, M., S. Nigam, and E. H. Berbery, 1998: Evolution of the North American monsoon
586 system. *J. Climate*, **11**, 2238-2257.

587 Bombardi, R. J., and L. M. V. Carvalho, 2009: IPCC Global coupled climate model simulations
588 of the South America Monsoon System. *Climate Dynamics* **33**, 893-916.

589 Bony, S., and J. L. Dufresne, 2005: Marine boundary layer clouds at the heart of tropical cloud
590 feedback uncertainties in climate models. *Geoph. Res. Letters*, **32**,
591 doi:10.1029/2005GL023851

592 Carvalho, L.M.V., Jones, C., Liebmann, B., 2002. Extreme precipitation events in Southeastern
593 South America and large-scale convective patterns in the South Atlantic Convergence Zone.
594 *J. Climate*, **15**, 2377–2394.

595 Carvalho, L. M. V., C. Jones, A. E. Silva, B. Liebmann, and P. L. S. Dias, 2011a: The South
596 American Monsoon System and the 1970s climate transition. *Int. Journal of Climatology*, **31**,
597 1248-1256, DOI: 1210.1002/joc.2147.

598 Carvalho, L. M. V., A. E. Silva, C. Jones, B. Liebmann, and H. Rocha, 2011b: Moisture
599 transport and Intraseasonal Variability in the South America Monsoon System. *Climate*
600 *Dynamics* **36**, 1865-1880, DOI 1810.1007/s00382-00010-00806-00382.

601 Carvalho, L. M. V., M. A. F. S. Dias, P. L. S. Dias, C. Jones, B. Liebmann, B. Bookhagen, and
602 A. E. Silva, 2012: Changes in the South American Monsoon System during 1948-2010.
603 *Submitted to J.Climate*

604 Cavalcanti, I. F. A., 2012: Large scale and synoptic features associated with extreme
605 precipitation over South America: A review and case studies for the first decade of the 21st
606 century. *Atmospheric Research*, **18**, 27-40.

607 Cherchi, A., A. Alessandri, S. Masina, and A. Navarra, 2011: Effects of increased CO₂ levels on
608 monsoons. *Clim. Dyn.*, **37**, 83-101.

609 Chou C., and J. D. Neelin, 2004: Mechanisms of global warming impacts on regional tropical
610 precipitation. *J. Climate* **17**, 2688–2701

611 Chou C, J. D. Neelin, C-A Chen, and J-Y Tu, 2009: Evaluating the “rich-get-richer” mechanism
612 in tropical precipitation change under global warming. *J Climate*, **22**, 1982–2005.

613 Dessler, A. E., and S. M. Davis, 2010: Trends in tropospheric humidity from reanalysis systems,
614 *J. Geophys. Res.*, **115**, D19127, doi:10.1029/2010JD014192.

615 Douglas, M. W., R. Maddox, K. Howard, and S. Reyes, 1993: The Mexican monsoon. *J.*
616 *Climate*, **6**, 1665-1667.

617 Forster P, and co-authors, 2007: Changes in atmospheric constituents and in radiative forcing. In:
618 Solomon S, Qin D, Manning M, Chen Z, Marquis M, Averyt KB, Tignor M, Miller HL (eds)
619 Climate change 2007: the physical science basis. contribution of working group I to the
620 fourth assessment report of the intergovernmental panel on climate change. Cambridge
621 University Press, Cambridge.

622 Fu, R. and W. Li, 2004: The influence of the land surface on the transition from dry to wet
623 season in Amazonia. *Theor. Appl. Climatol.*, **78**, 97-110, DOI 10.1007/s00704-004-0043-x.

624 Gan, M. A., V. E. Kousky, C. F. Ropelewski, 2004: The South America monsoon circulation and
625 its Relationship to Rainfall over West-Central Brazil. *J. Climate*, **17**, 47–66.

626 Gutzler, D. S., 200: Covariability of spring snowpack and summer rainfall across the southwest
627 United States. *J. Climate*, **13**, 4018-4027.

628 Gutzler, D. S., and J. W. Preston, 1997: Evidence for a relationship between spring snow cover
629 and summer rainfall in New Mexico. *Geophys. Res. Lett*, **24**, 2207-2210.

630 Higgins, R. W., Y. Chen, and A. F. Douglas, 1999: Interannual variability of the U. S. summer
631 precipitation regime with emphasis on the southwestern monsoon. *J. climate*, **11**, 2582-2606

632 Kalnay, E., and Coauthors, 1996: The NCEP-NCAR 40 Year Reanalysis Project. *Bulletin of the*
633 *American Meteorological Society*, **77**, 437-471.

634 Kistler, R., and Coauthors, 2001: The NCEP-NCAR 50-Year Reanalysis: Monthly Means CD-
635 ROM and Documentation. *Bulletin of the American Meteorological Society*, **82**, 247-267.

636 Kodama, Y. M., 1992: Large-Scale Common Features of Subtropical Precipitation Zones (the
637 Baiu Frontal Zone, the SPCZ, and the SACZ) .1. Characteristics of Subtropical Frontal
638 Zones. *Journal of the Meteorological Society of Japan*, **70**, 813-836.

639 Jones, C. and L. M. V. Carvalho, 2012: Climate change in the South American Monsoon
640 System: present climate and CMIP5 projections. *J. Climate (submitted)*.

641 Marengo, J. A., and Coauthors, 2010: Review: Recent developments on the South American
642 monsoon system. *International Journal of Climatology*, DOI: 10.1002/joc.2254

643 Marengo, J. A, B. Liebmann, V. Kousky, N. Filizola, and I. Wainer, 2001: On the onset and end
644 of the rainy season in the Brazilian Amazon basin. *J. Climate*, **14**, 833–852.

645 Mechoso, C. R., A. W. Robertson, C. F. Ropelewski, A. M. Grimm, 2005: The American
646 Monsoon Systems: An Introduction. C.-P. Chang, B. Wang and N.-C. G. Lau, Eds WMO/TD
647 No. 1266 (TMRP Report No. 70), 197-206.

648 Moss, R. H., and Coauthors, 2010: The next generation of scenarios for climate change research
649 and assessment. *Nature*, **463**, 747-756

650 Raia, A, I. F. A. Cavalcanti, 2008: The Life Cycle of the South American Monsoon System. *J.*
651 *Climate*, **21**, 6227–6246

652 Rickenbach, T. M., R. Nieto- Ferreira, R. P. Barnhill, S. W. Nesbitt, 2011. Regional contrasts of
653 mesoscale convective system structure prior to and during monsoon onset across South
654 America, *J. Climate*, **24**, 3753-3763.

655 Richter I., S-P Xie , 2008: Muted precipitation increase in global warming simulations: A surface
656 evaporation perspective. *J Geophys Res*, **113**:D24118. doi:10.1029/2008JD010561.

657 Rodionov, S. N., 2004: A sequential algorithm for testing climate regime shifts. *Geophys. Res.*
658 *Lett.*, 31: L09204, DOI:09210.01029/02004GL-019448, 012004.

659 Ropelewski, C.F, D.S. Gutzler, R.W. Higgins, and C. R. Mechoso, 2005: The North American
660 Monsoon System, Proc. Third Int. Workshop on Monsoons (IWM-III), Hangzhou, China, 2-6
661 Nov. 2004.

662 Saha, S., and Coauthors, 2010: The NCEP Climate Forecast System Reanalysis. *Bulletin of the*
663 *American Meteorological Society*, **91**, 1015-1057.

664 Samanta, A., and co-authors, 2011: Comment on "Drought-induced reduction in global terrestrial
665 net primary production from 2000 through 2009", *Science*, 333, 6046, doi:
666 10.1126/science.1199048

667 Seth, A., M. Rojas, and S. A. Rauscher, 2010: CMIP3 projected changes in the annual cycle of
668 the South American Monsoon. *Climatic Change*, **98**, 331-357.

669 Sheffield, J. and co-authors, 2012: North American Climate in CMIP5 Experiments: Part II:
670 Evaluation of 20th Century Intra-Seasonal to Decadal Variability. *J. Climate* (submitted)

671 Silva, A. E., and L. M. V. Carvalho, 2007: Large-scale index for South America Monsoon
672 (LISAM). *Atmospheric Science Letters*, **8**, 51-57.

673 Silva Dias, M. A. F., J. Dias, L. M. V. Carvalho, E. D. Freitas, and P. L. S. Dias, 2012: Changes
674 in extreme daily rainfall for São Paulo, Brazil. *Climatic Change*, DOI 10.1007/s10584-
675 10012-10504-10587.

676 Taylor, K. E., R. J. Stouffer, and G. A. Meehl, 2011: An Overview of CMIP5 and the
677 Experiment Design. *Bulletin of the American Meteorological Society*, **93**, 485-498.

678 Vera C, W. Higgins, J. Amador, T. Ambrizzi, R. Garreaud, D. Gochis, D. Gutzler, D.
679 Lettenmaier, J. Marengo, C. R. Mechoso, J. Noguez-Paegle, P. L. Silfa Dias, and C. Zhang,
680 2006: Toward a unified view of the American monsoon systems. *J Climate*, **19**, 4977–5000

681 Vera C. S. , and G. Silvestri , 2009: Precipitation interannual variability in South America from
682 the WCRP-CMIP3 Multi-model dataset. *Climate Dynamics* **32**, 1003–1014.

683 Wang, H., and R. Fu, 2002: Cross-equatorial flow and seasonal cycle of precipitation over South
684 America. *J. Climate*, **15**, 1591–1608.

685 Yuter, S. E, Y. L. Serra, and R. A. Houze Jr., 2000: The 1997 Pan American Climate Studies
686 Tropical Eastern Pacific Process Study. Part II: Stratocumulus region. *Bull. Amer. Meteor.*
687 *Soc.*, **81**, 483–499.

688

689 Table 1. List of CMIP5 models used in this study. All eleven models were used for analyses of
690 the historical experiment. Symbol “*” indicates models analyzed for the RCP8.5 scenario.

	Modeling Center (or Group)	Institute ID	Model Name
1	Canadian Centre for Climate Modelling and Analysis	CCCMA	CanESM2*
2	Centre National de Recherches Meteorologiques / Centre Europeen de Recherche et Formation Avancees en Calcul Scientifique	CNRM-CERFACS	CNRM-CM5
3	Commonwealth Scientific and Industrial Research Organization in collaboration with Queensland Climate Change Centre of Excellence	CSIRO-QCCCE	CSIRO-Mk3.6.0
4	NOAA Geophysical Fluid Dynamics Laboratory	NOAA GFDL	GFDL-ESM2M*
5	Institute for Numerical Mathematics	INM	INM-CM4
6	Institut Pierre-Simon Laplace	IPSL	IPSL-CM5A-LR
7	Atmosphere and Ocean Research Institute (The University of Tokyo), National Institute for Environmental Studies, and Japan Agency for Marine-Earth Science and Technology	MIROC	MIROC4h
8	Max Planck Institute for Meteorology	MPI-M	MPI-ESM-LR*
9	Meteorological Research Institute	MRI	MRI-CGCM3*
10	Norwegian Climate Centre	NCC	NorESM1-M*
11	Met Office Hadley Centre	MOHC	HadCM3

691

692

693 Table-2. 85th percentiles (1951-2005) of the historical runs for South America (SA) and North
694 America (NA) and for NCEP/NCAR and CFSR reanalyses*. The 85th percentile for CFSR was
695 calculated from 1979-2005. The symbol “__” indicates that the quantity is not available for the
696 model.

	South America (DJF)		North America (JJA)	
Model Name	T850 (°C)	Q850 (g/kg)	T850 (°C)	Q850 (g/kg)
CFSR*	18.88	12.23	20.21	10.37
NCEP/NCAR*	18.09	11.87	20.00	9.70
CanESM2	21.40	12.33	23.40	9.31
CSIRO-Mk3.6.0	21.16	12.22	22.77	11.05
MIROC4H	20.62	12.07	21.75	9.63
HadCM3	19.40	_____	19.55	_____
GFDL-ESM2M	18.89	11.46	18.28	9.37
IPSL-CM5A-LR	18.77	10.98	18.52	8.39
CNRM-CM5	18.62	11.84	20.68	9.33
NorESM1-M	18.43	11.63	19.48	9.64
MPI-ESM-LR	18.07	11.89	19.21	10.16
MRI-CGCM3	17.80	12.92	17.57	10.09
INM-CM4	17.22	11.65	19.55	9.18

697

698

699 **Figure Captions:**

700 Figure 1. Decadal variation of the T850 85th percentile (T850_{p85}) during DJF for the historic
 701 simulations (1951-2005). Values of the T850_{p85} were calculated over SA (see Table-2): a)
 702 NCEP/NCAR, b) CFSR, c) GFDL-ESM2M, d) MRI-CGCM3, e) MPI-ESM-LR, f) NorESM1-
 703 M, g) INM-CM4, h) IPSL-CM5A-LR, i) MIROC4h, j) HadCM3, k) CanESM2, l) CSIRO-
 704 Mk3.6.0, m) CNRM-CM5. For NCEP/NCAR (a) and all CMIP5 models, averages were taken in
 705 the following decades: 1956-1965 (black solid line); 1966-1975 (dark blue dashed line); 1976-
 706 1985 (light blue solid line); 1986-1995 (dark magenta dashed line); 1996-2005 (red solid line).
 707 Decadal averages for CSFR (b) were obtained for the periods 1979-1985 (black solid line), 1986-
 708 1995 (blue dashed line), 1996-2005 (red solid line). Grey shade indicates topography above
 709 1500m and thick black dashed lines show the 1500m height (continues).

710 Figure 2. a) Interannual variability of T850_{p85} over SA during DJF for NCEP/NCAR and CFSR
 711 reanalyses and the CMIP5 historic simulations (1951-2005); b) interannual variability of T850_{p85}
 712 after removing the intercept of the linear fit: NCEP/NCAR, CFSR, CMIP5 ensemble mean,
 713 maximum and minimum; c) Interannual variability of the fraction of SA with temperature greater
 714 or equal T850_{p85} (%) calculated for the 1951-2005 period (1979-2005 for CFSR) . All curves are
 715 9-year moving averages. The CMIP5 models in a) are indicated in the legend.

716 Figure 3. The same as Fig. 1 but for Q850_{p85} (values shown in Table-2). The following models
 717 are analyzed: a) NCEP/NCAR, b) CFSR, c) GFDL-ESM2M, d) MRI-CGCM3, e) MPI-ESM-LR,
 718 f) NorESM1-M, g) INM-CM4, h) IPSL-CM5A-LR, i) MIROC4h, j) CanESM2, k) CSIRO-
 719 Mk3.6.0, l) CNRM-CM5. HadCM3 is not examined because of the unavailability of daily
 720 specific humidity at 850hPa (continues).

721 Figure 4. a) Interannual variability of Q850_{p85} over SA during DJF for NCEP/NCAR and CFSR
 722 reanalyses and the CMIP5 historic simulations (1951-2005); b) interannual variability of Q850_{p85}
 723 CMIP5 ensemble mean, maximum and minimum and NCEP/NCAR and CFSR reanalyses; c)
 724 Interannual variability of the fraction of SA with specific humidity greater or equal Q850_{p85} (%)
 725 calculated for the 1951-2005 period. All curves are 9-year moving averages. The CMIP5 models
 726 in a) are indicated in the legend.

727 Figure 5. The same as Fig. 1 but for NA during JJA.

728 Figure 6. The same as Fig. 2 but for NA during JJA.

729 Figure 7. The same as Fig. 3 but for NA during JJA.

730 Figure 8. The same as Fig. 4 but for NA during JJA.

731

Figure 9. Decadal variation of the T850 85th percentile (T850_{p85}) during DJF for the RCP8.5 simulations (2006-2095). Values of the T850_{p85} were calculated over SA for the historic run (see Table-2): a) GFDL-ESM2M, b) MRI-CGCM3, c) MPI-ESM-LR, d) INM-CM4, e) NorESM1-M, f) CanESM2 . Colors and line patterns represent different decades as indicated in the legend of the figure. Grey shade indicates topography above 1500m and thick black dashed lines show the 1500m height (continues).

Figure 10. a) CMIP5 historic simulations and RCP8.5 ensemble mean, maximum and minimum projections of T850_{p85} anomalies (intercept of the linear fit removed) over SA during DJF.; b) Fraction of SA (%) with T850 greater or equal T850_{p85} in the historic and RCP8.5 simulations (CMIP5 ensemble mean, maximum and minimum) during DJF. NCEP/NCAR and CFSR are also included (1955-2006). Curves are 9-year moving averages.

Figure 11. Decadal variation of the Q850 85th percentile (Q850_{p85}) during DJF for the RCP8.5 simulations (2006-2095). Values of the Q850_{p85} were calculated over SA for the historic run (see Table-2): a) GFDL-ESM2M, b) MRI-CGCM3, c) MPI-ESM-LR, d) NorESM1-M, e) CanESM2. Colors and line patterns represent different decades as indicated in the legends of the figure. Grey shade indicates topography above 1500m and thick black dashed lines show the 1500m height (continues).

Figure 12. a) CMIP5 historic simulations and RCP8.5 projections ensemble mean, maximum and minimum of Q850_{p85} over SA during DJF.; b) Fraction of SA (%) with Q850 greater or equal Q850_{p85} in the historic and RCP8.5 simulations (ensemble mean, maximum and minimum) during DJF. NCEP/NCAR and CFSR are also included (1955-2006). Curves are 9-year moving averages.

Figure 13. The same as Fig. 9 but for NA and JJA.

Figure 14. The same as Fig. 10 but for NA and JJA.

Figure 15. The same as Fig. 11 but for NA and JJA.

Figure 16. The same as Fig. 12 but for NA and JJA.

Table Captions:

Table 1. List of CMIP5 models used in this study. All eleven models were used for analyses of the historical experiment. Symbol “*” indicates models analyzed for the RCP8.5 scenario

Table-2. 85th percentiles (1951-2005) of the historical runs for South America (SA) and North America (NA) and for NCEP/NCAR and CFSR reanalyses*. The 85th percentile for CFSR was calculated from 1979-2005. The symbol “—” indicates that the quantity is not available for the model.

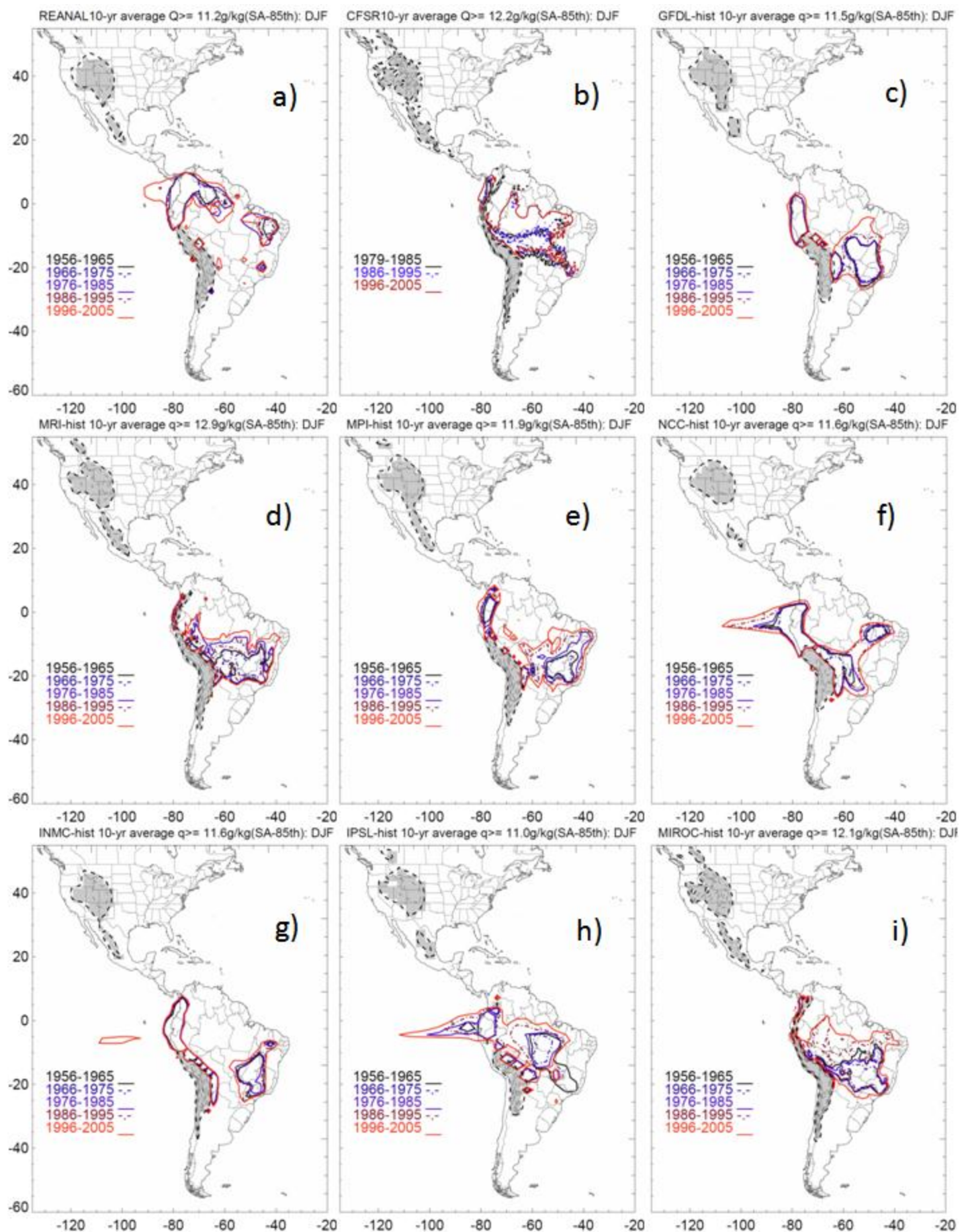


Figure 1 (continues)

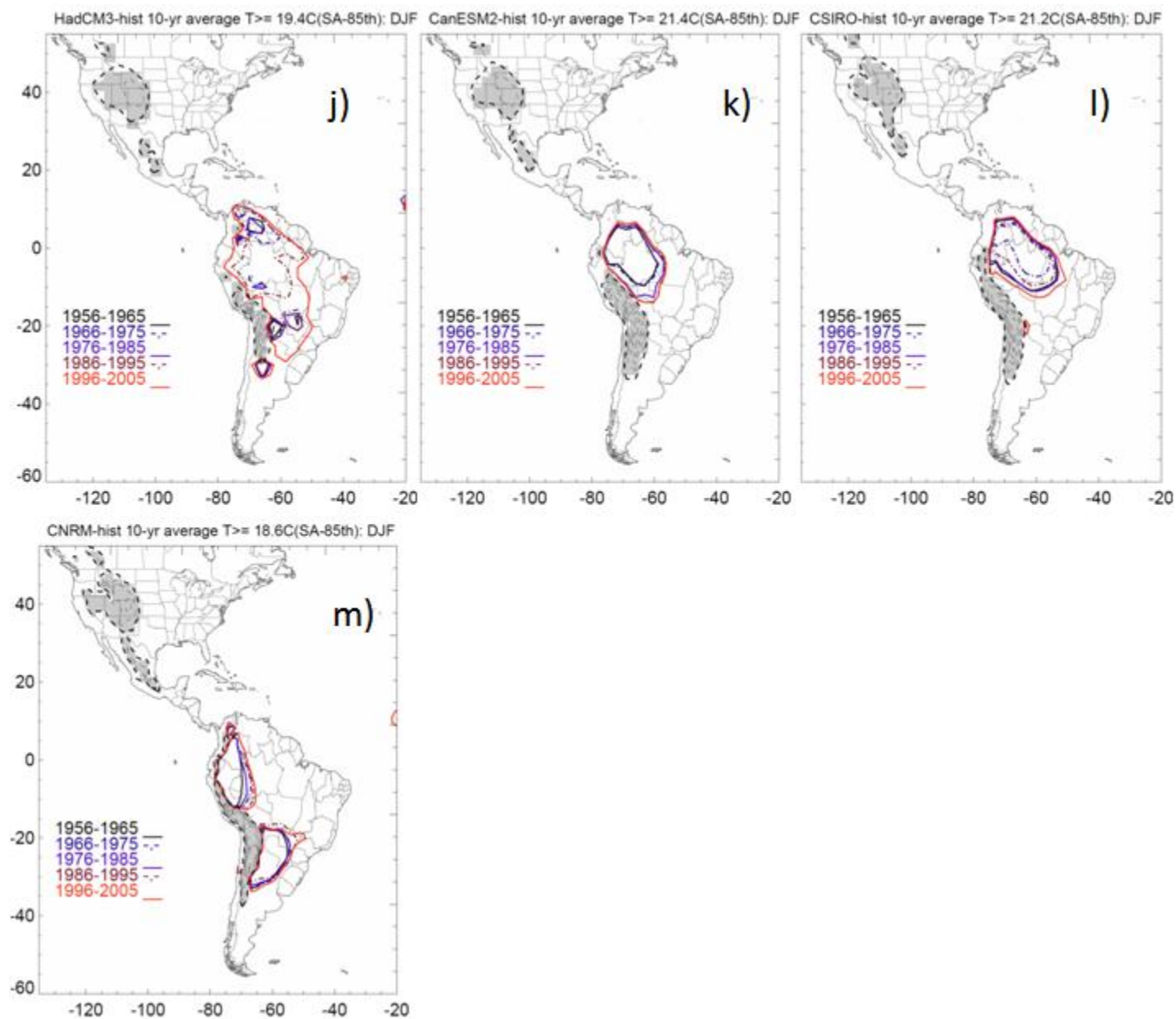


Figure 1 (continued)

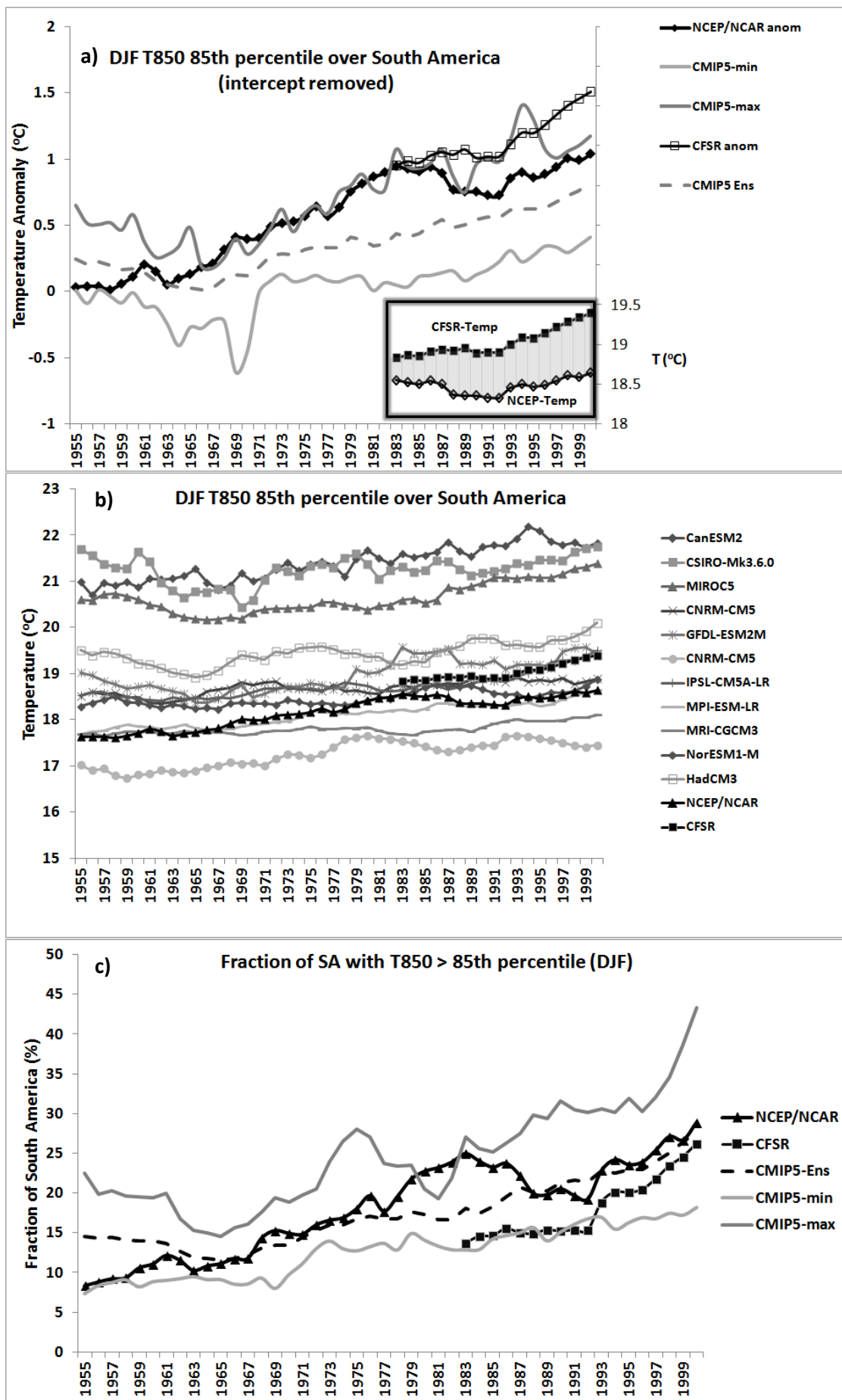


Figure 2.

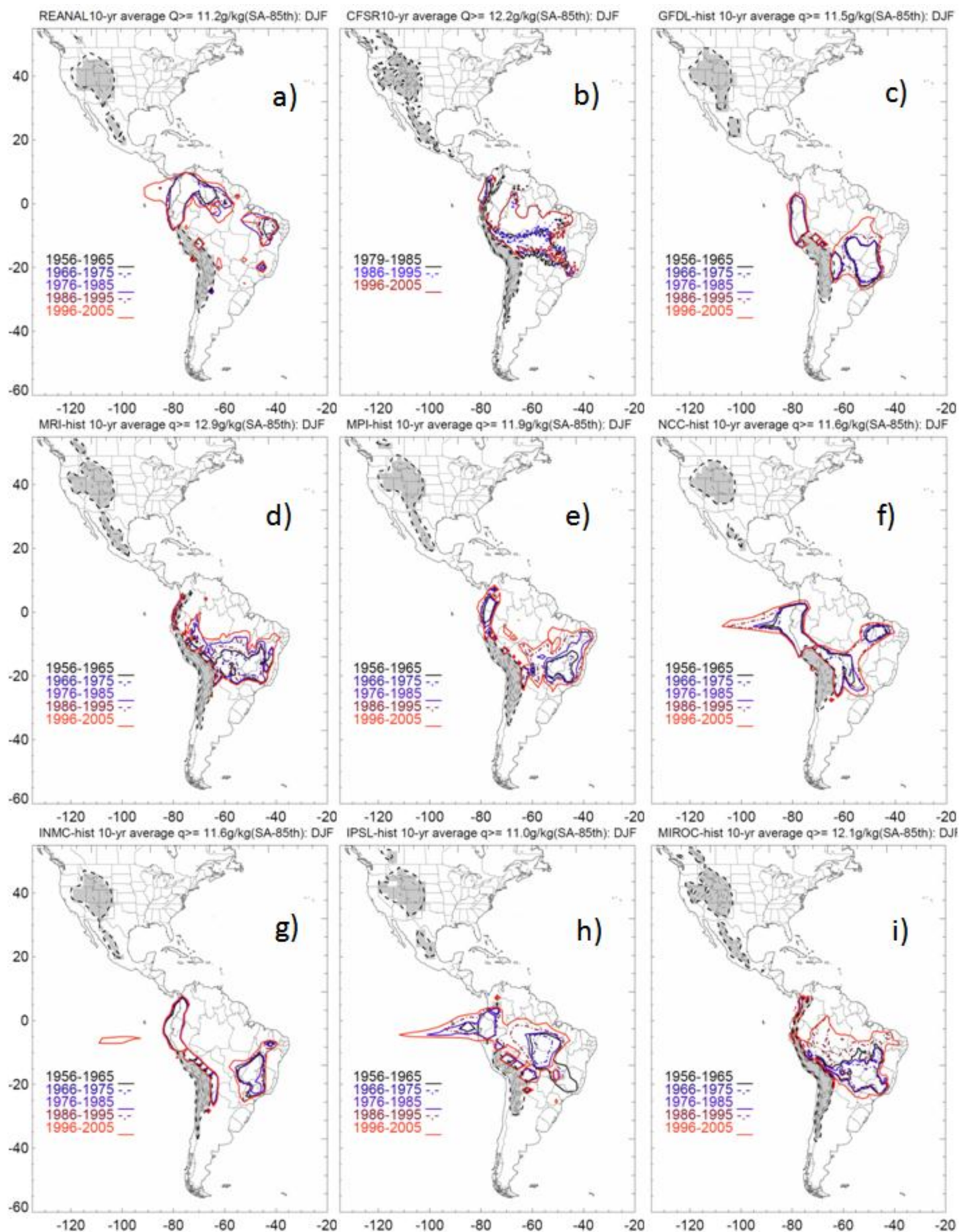


Figure 3 (continues)

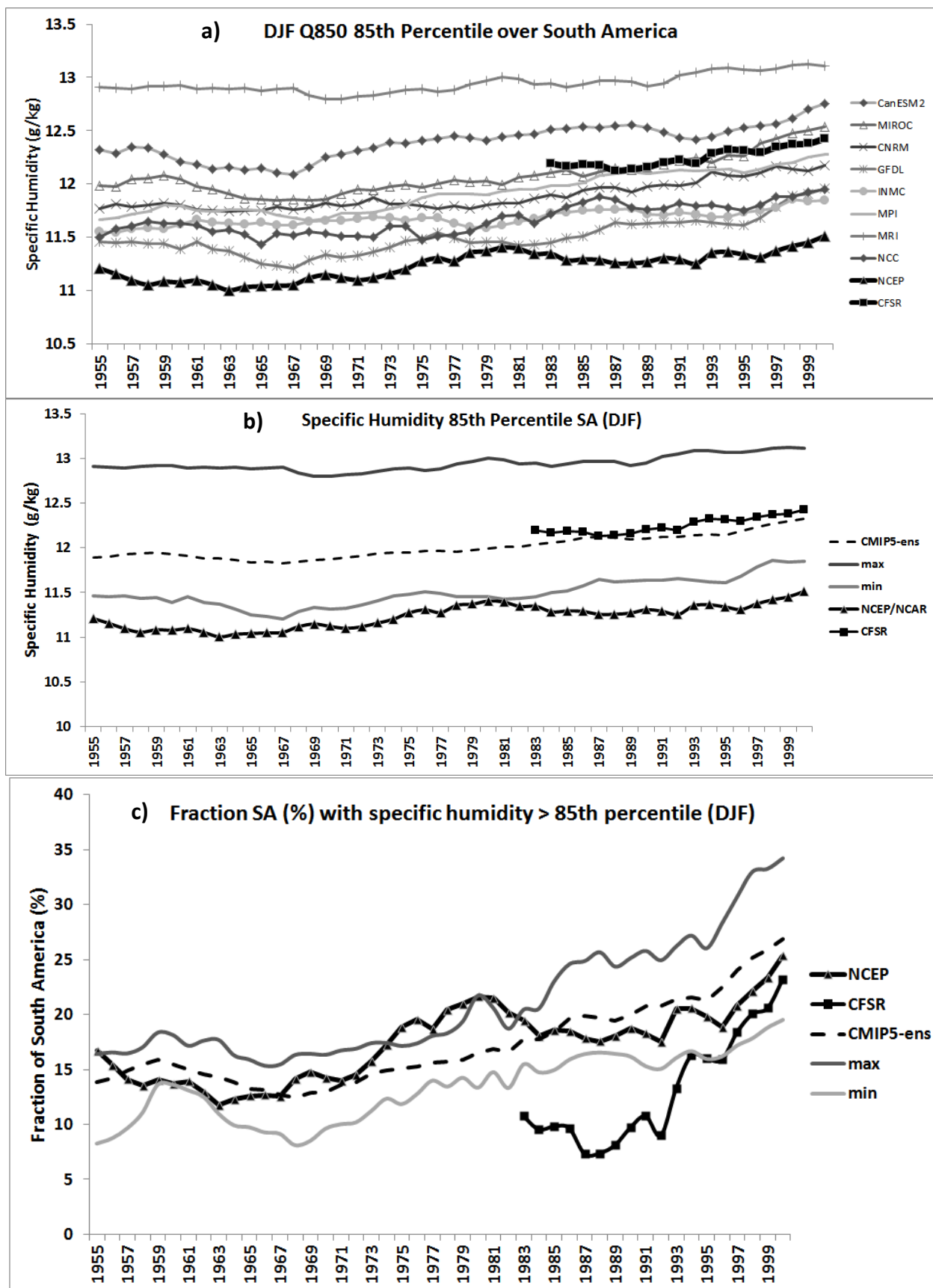


Figure 4

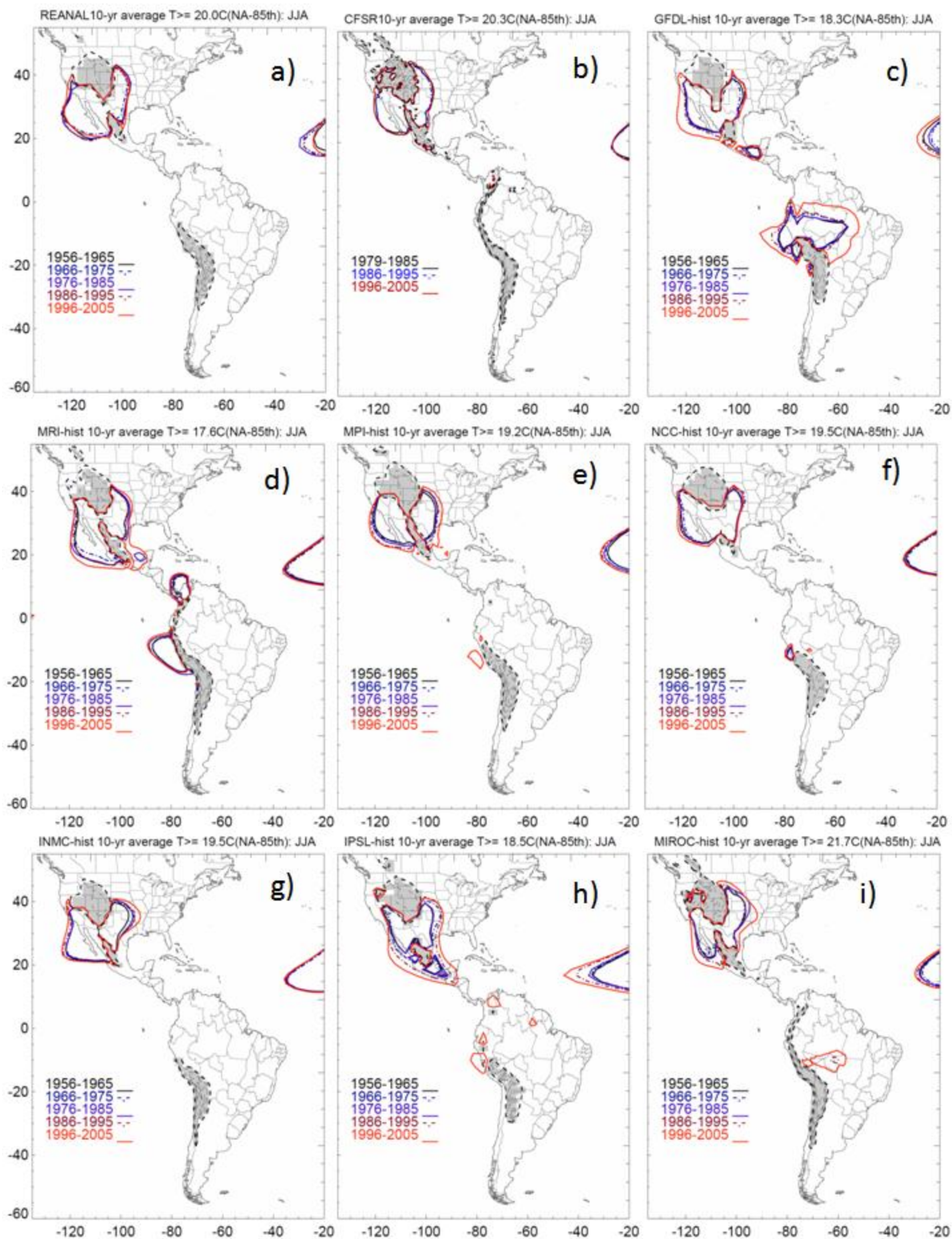


Figure 5 (continues)

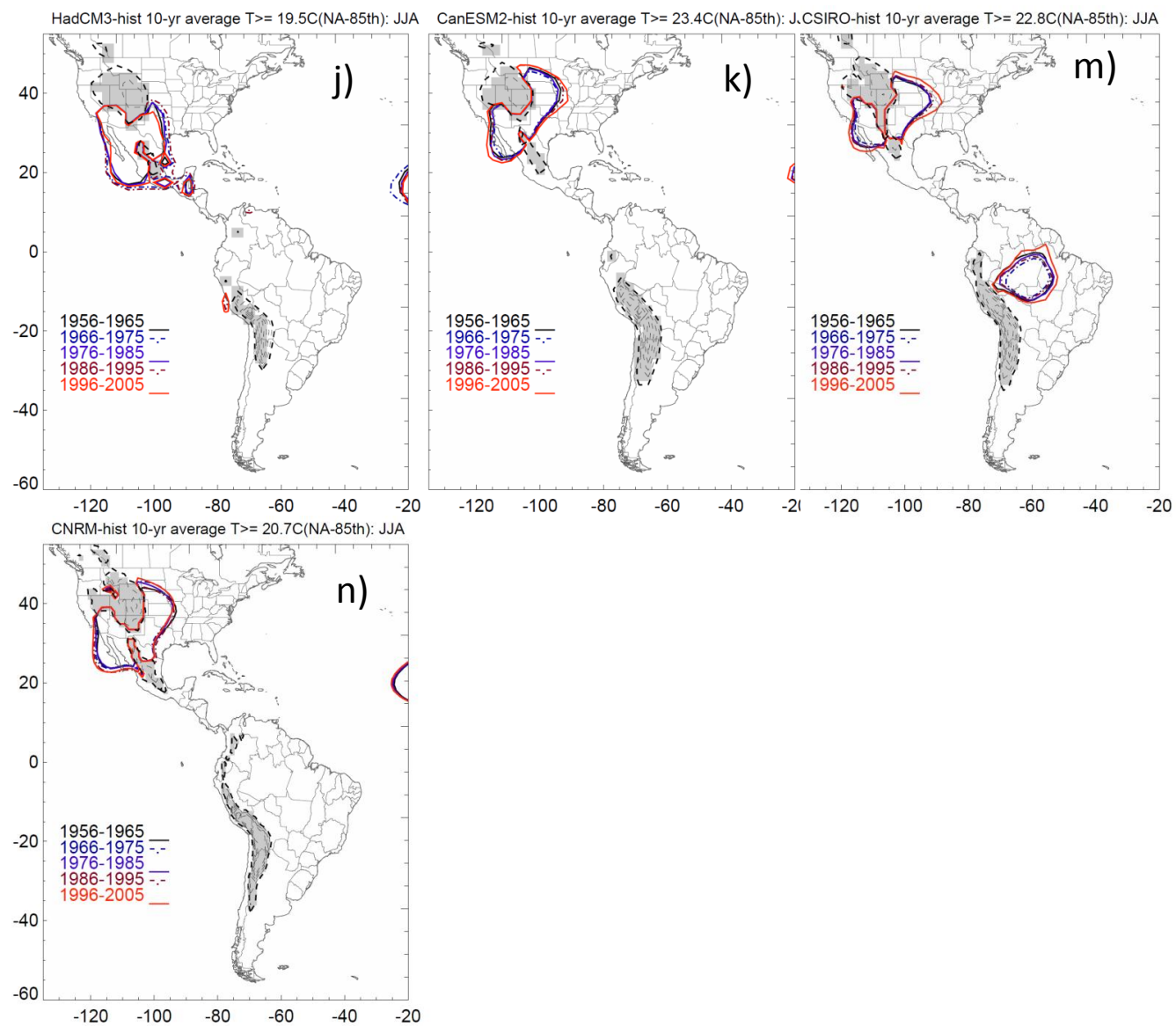


Figure 5 (continued)

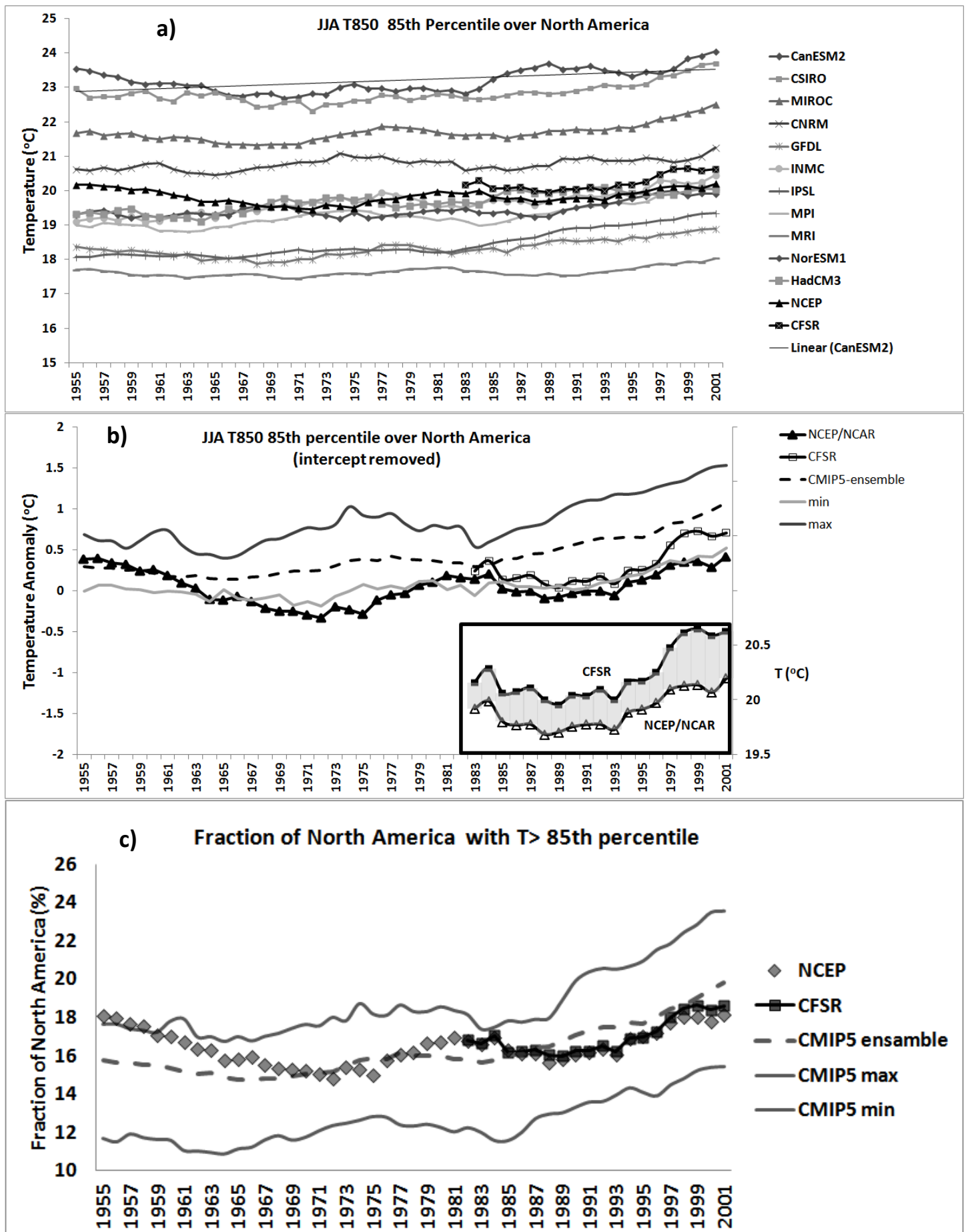


Figure 6

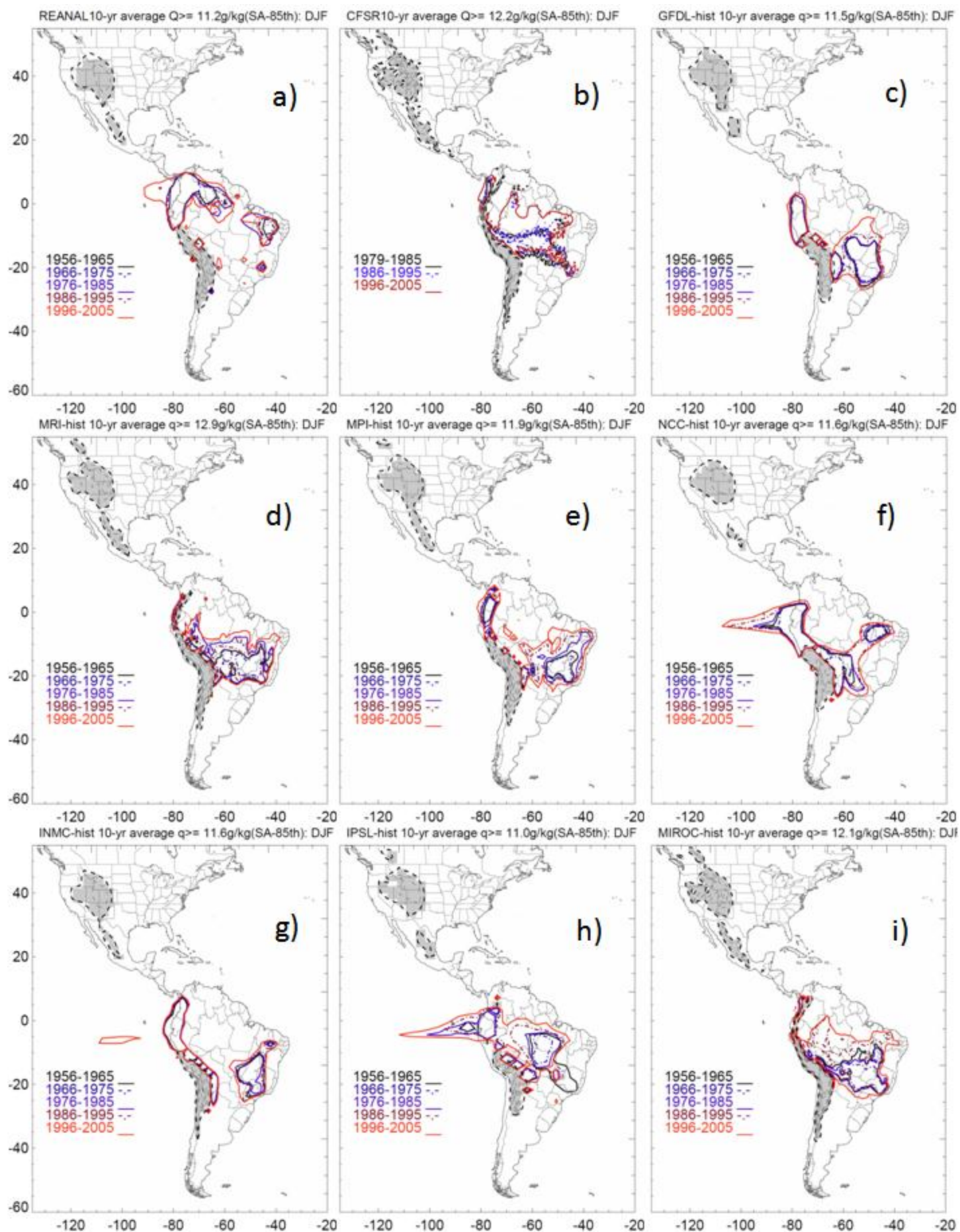


Figure 7 (continues)

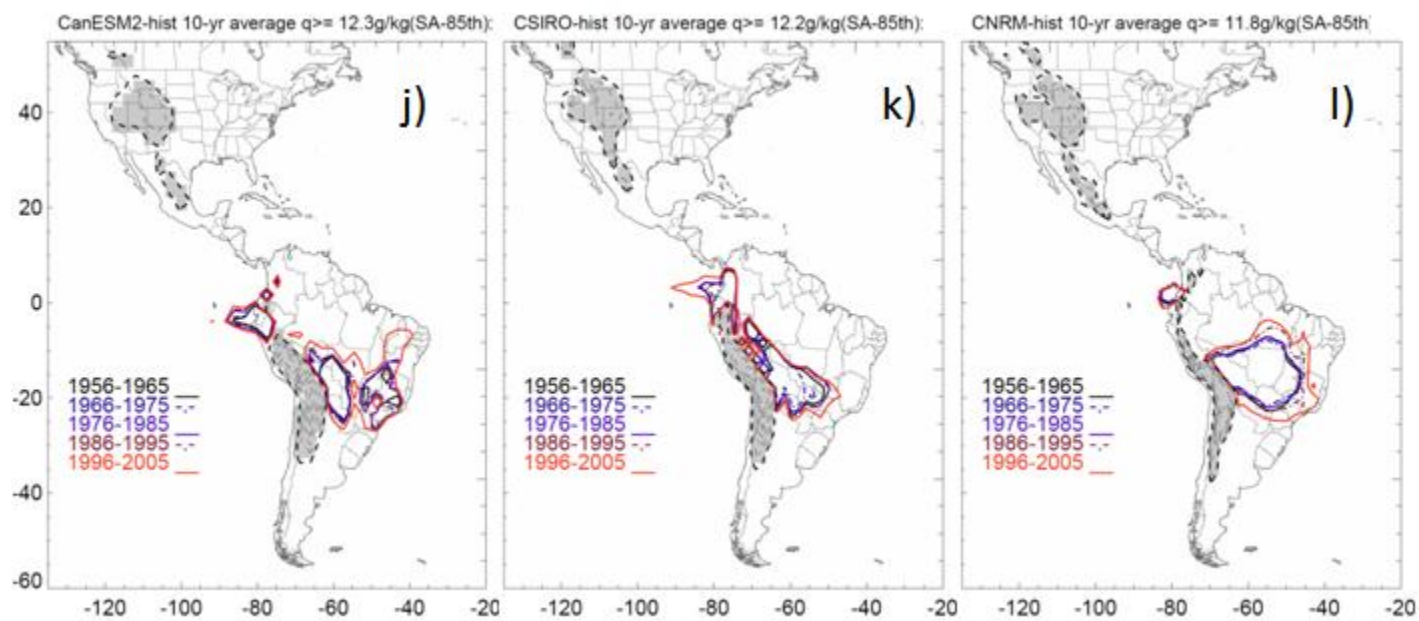


Figure 7 (continued)

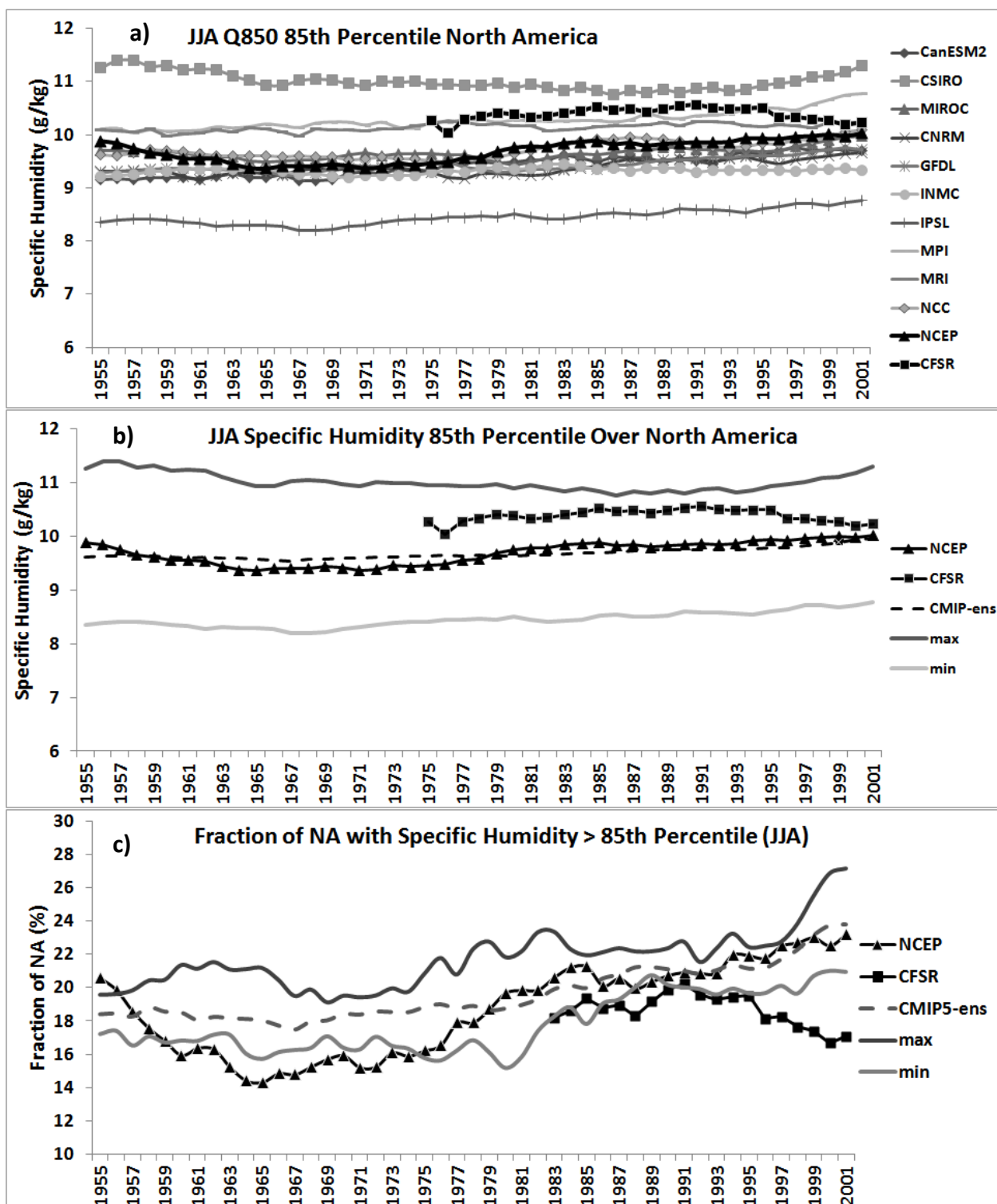


Figure 8

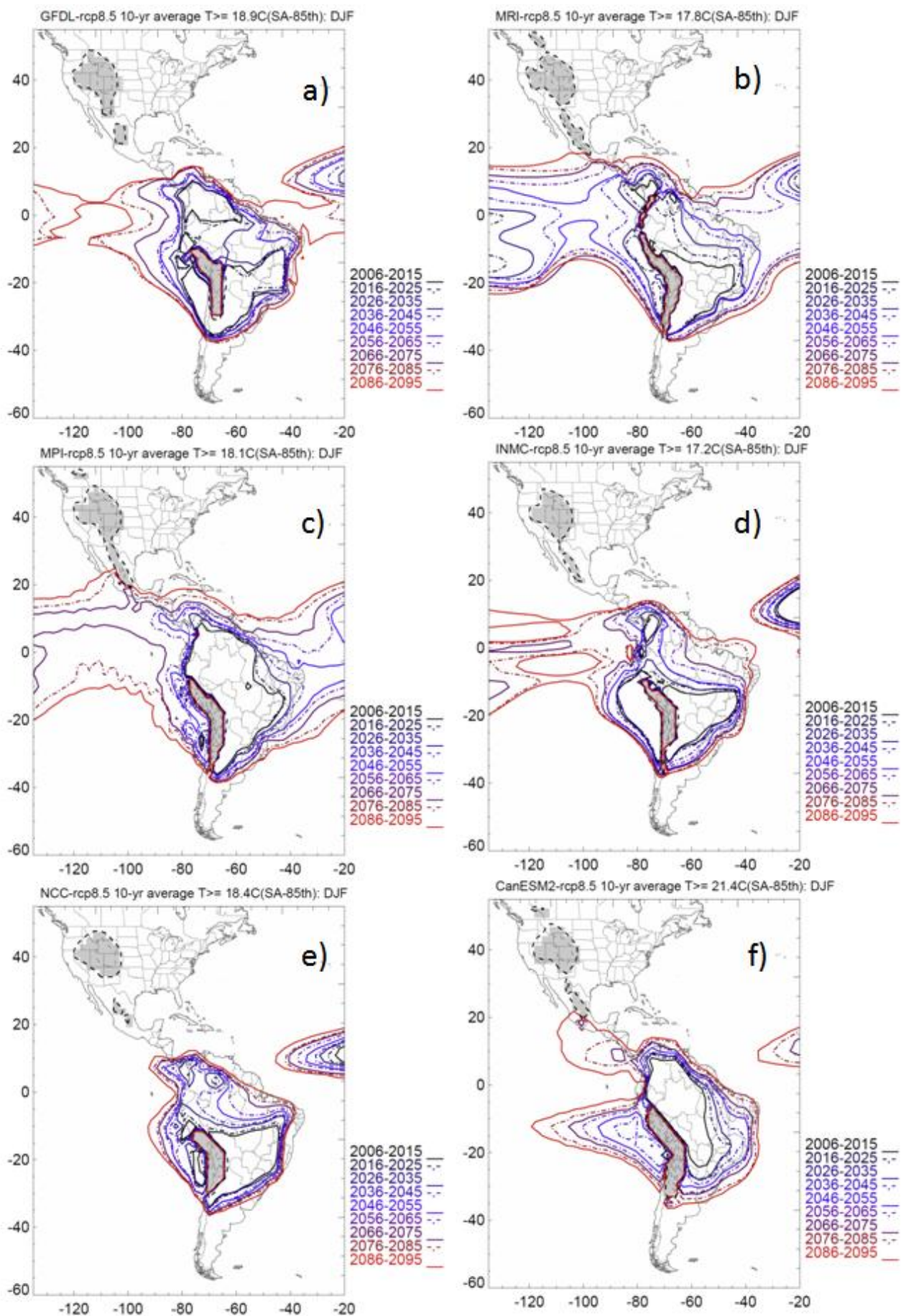


Figure 9

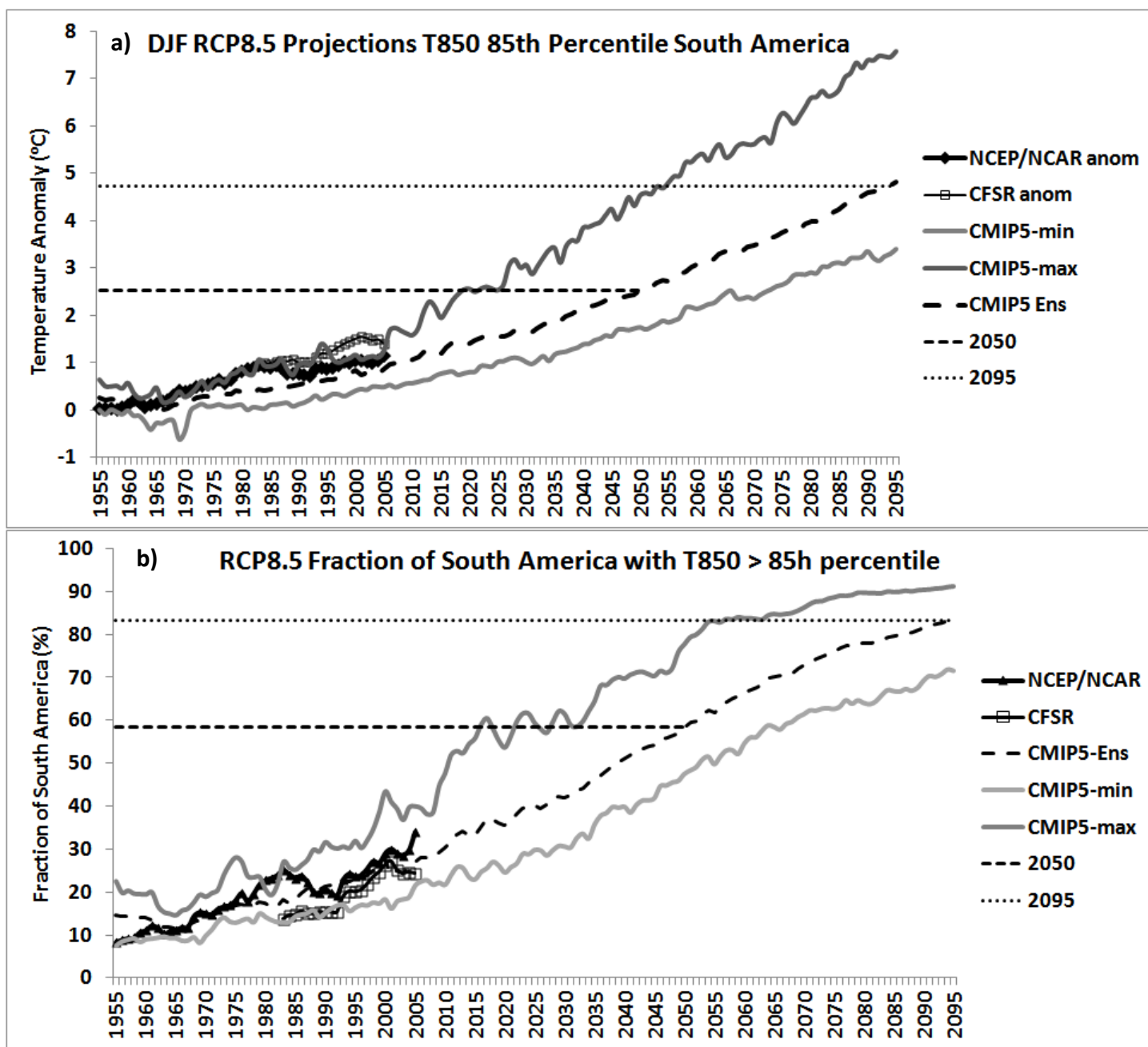


Figure 10

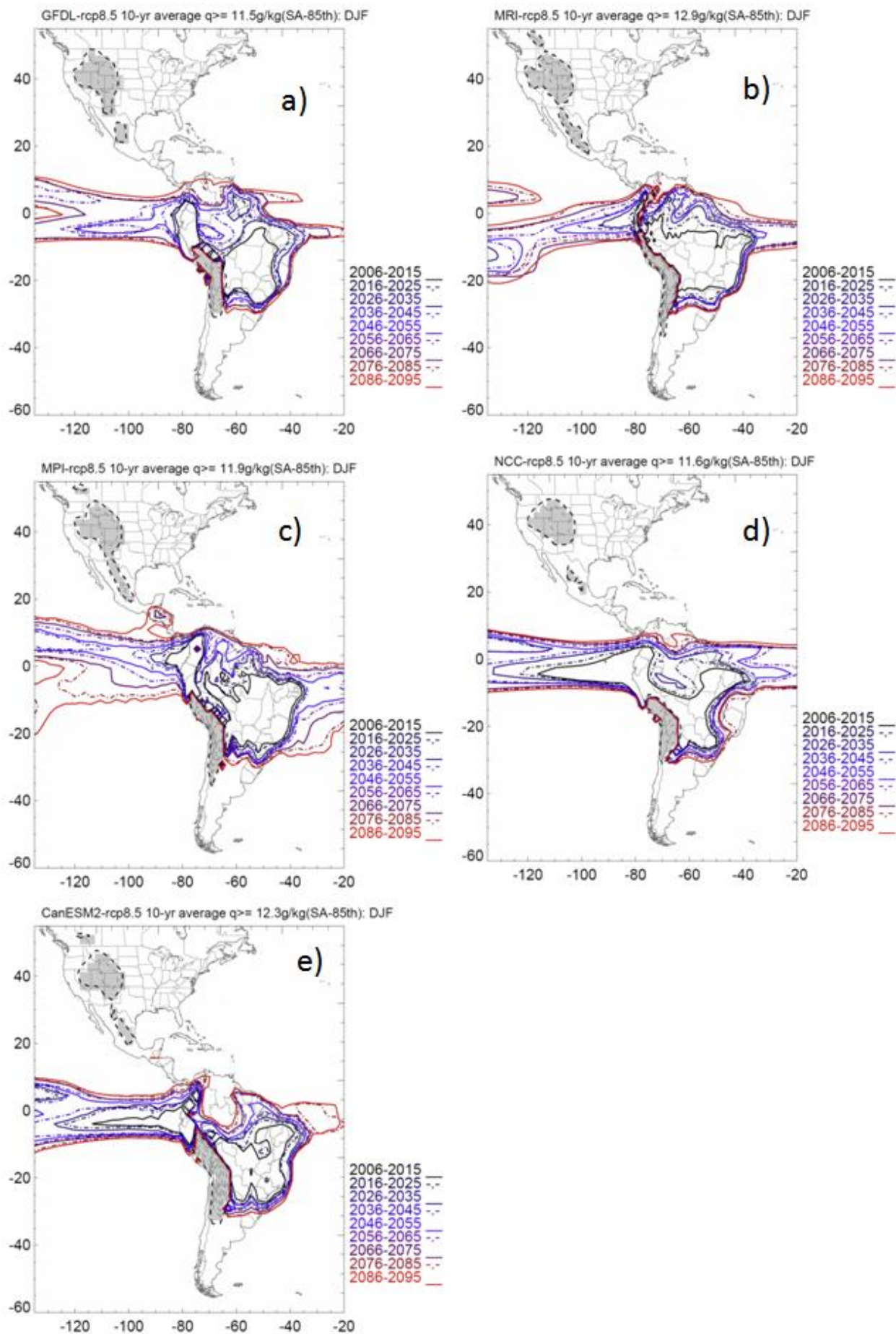


Figure 11

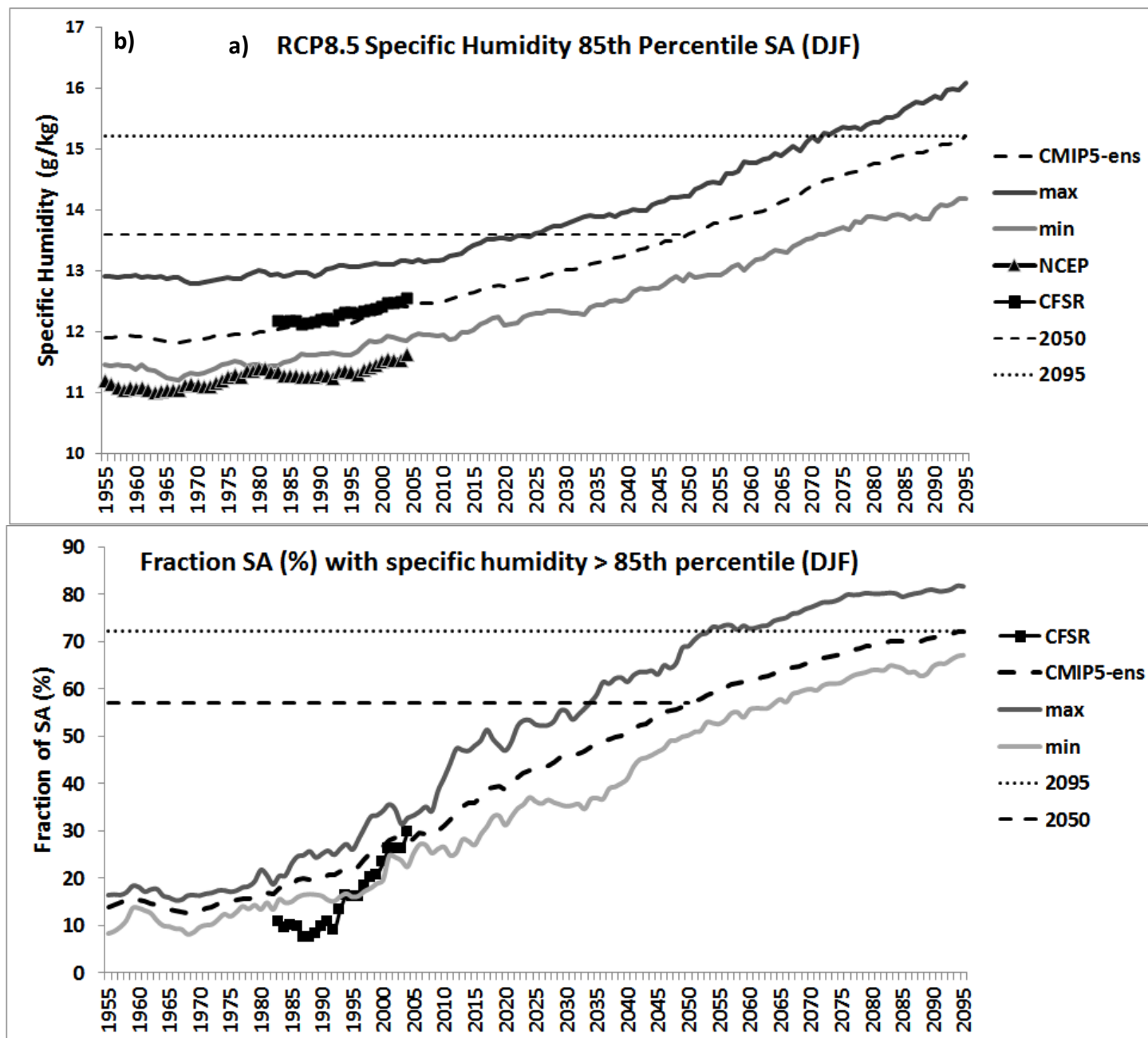


Figure 12

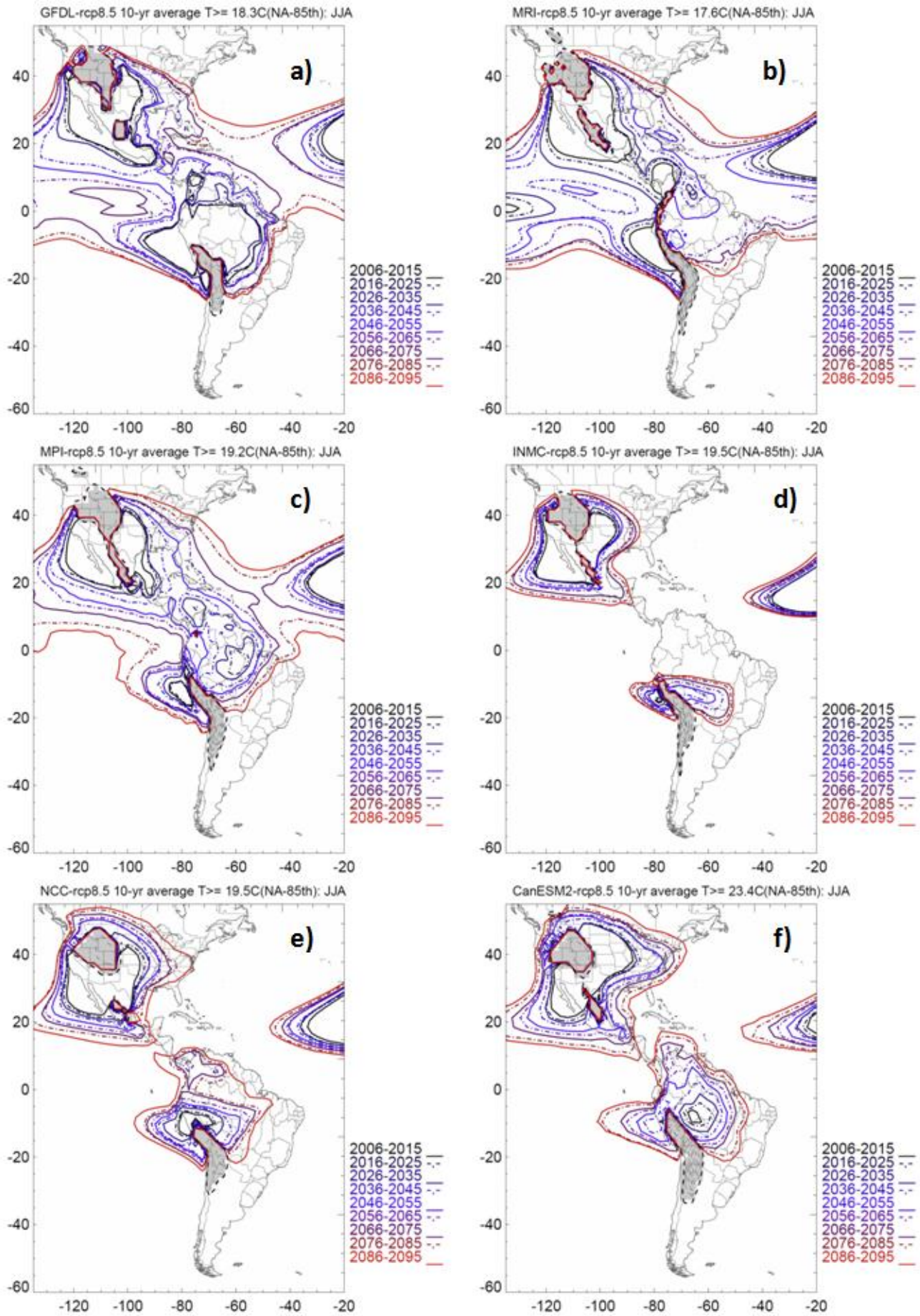


Figure 13

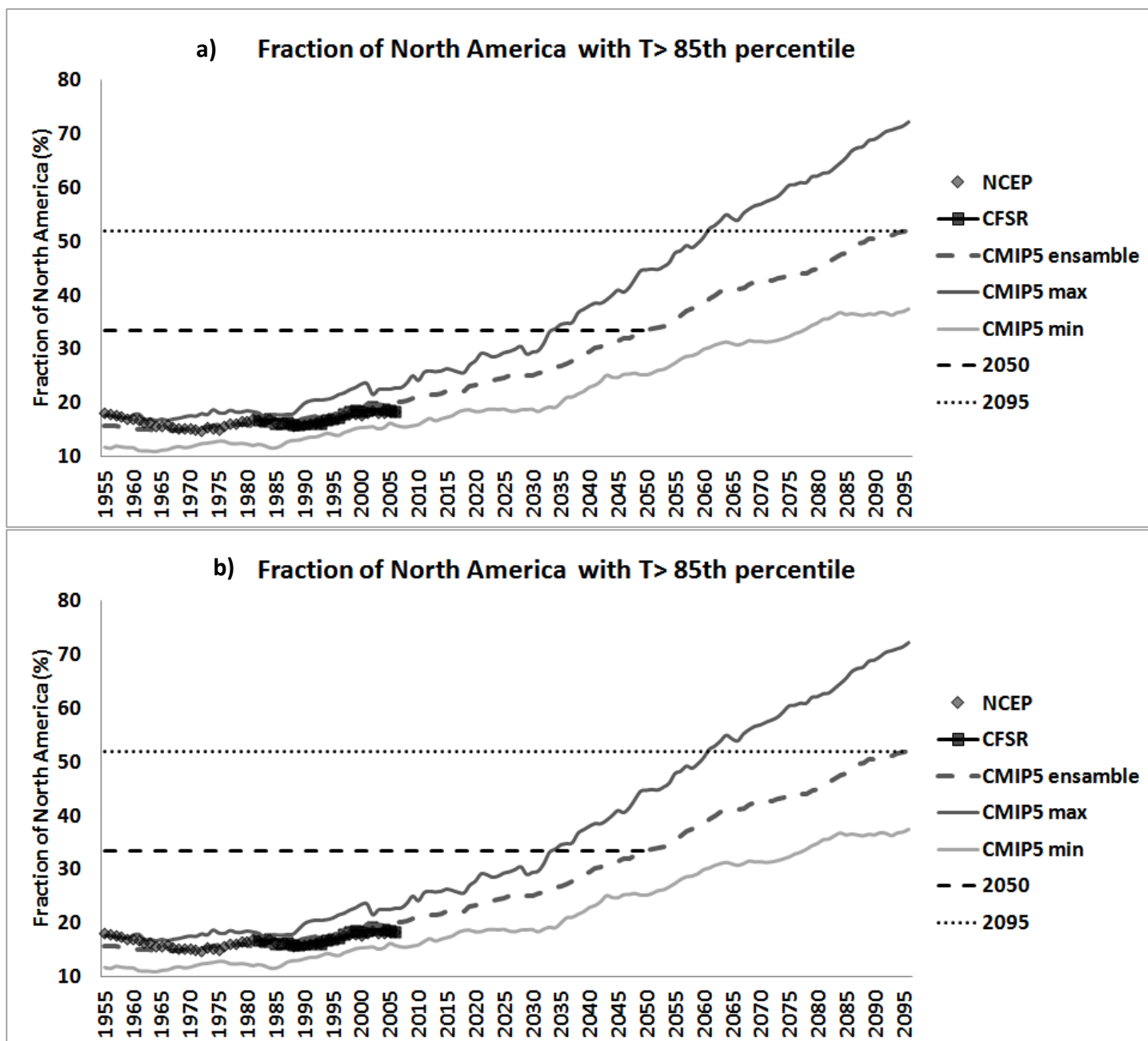


Figure 14

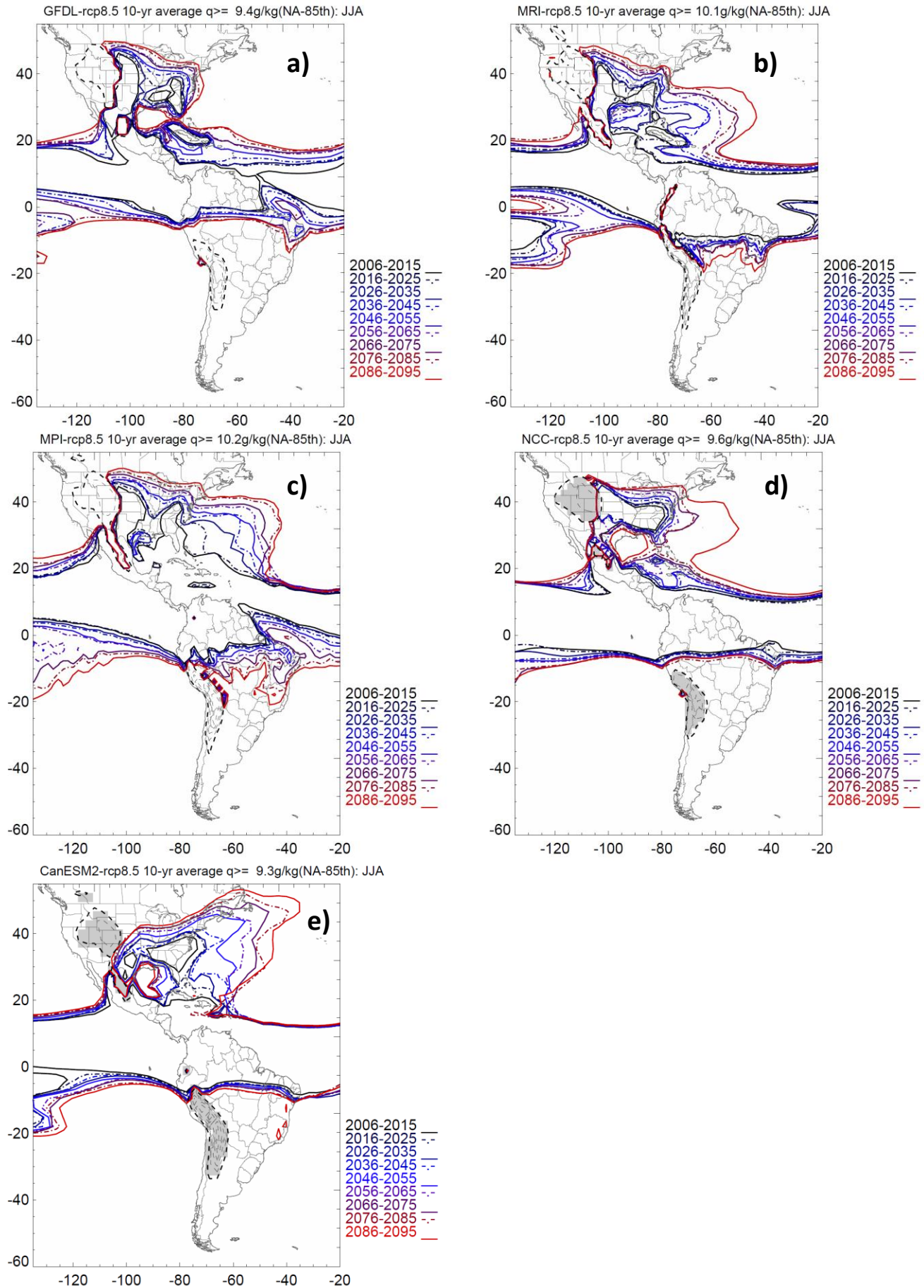


Figure 15

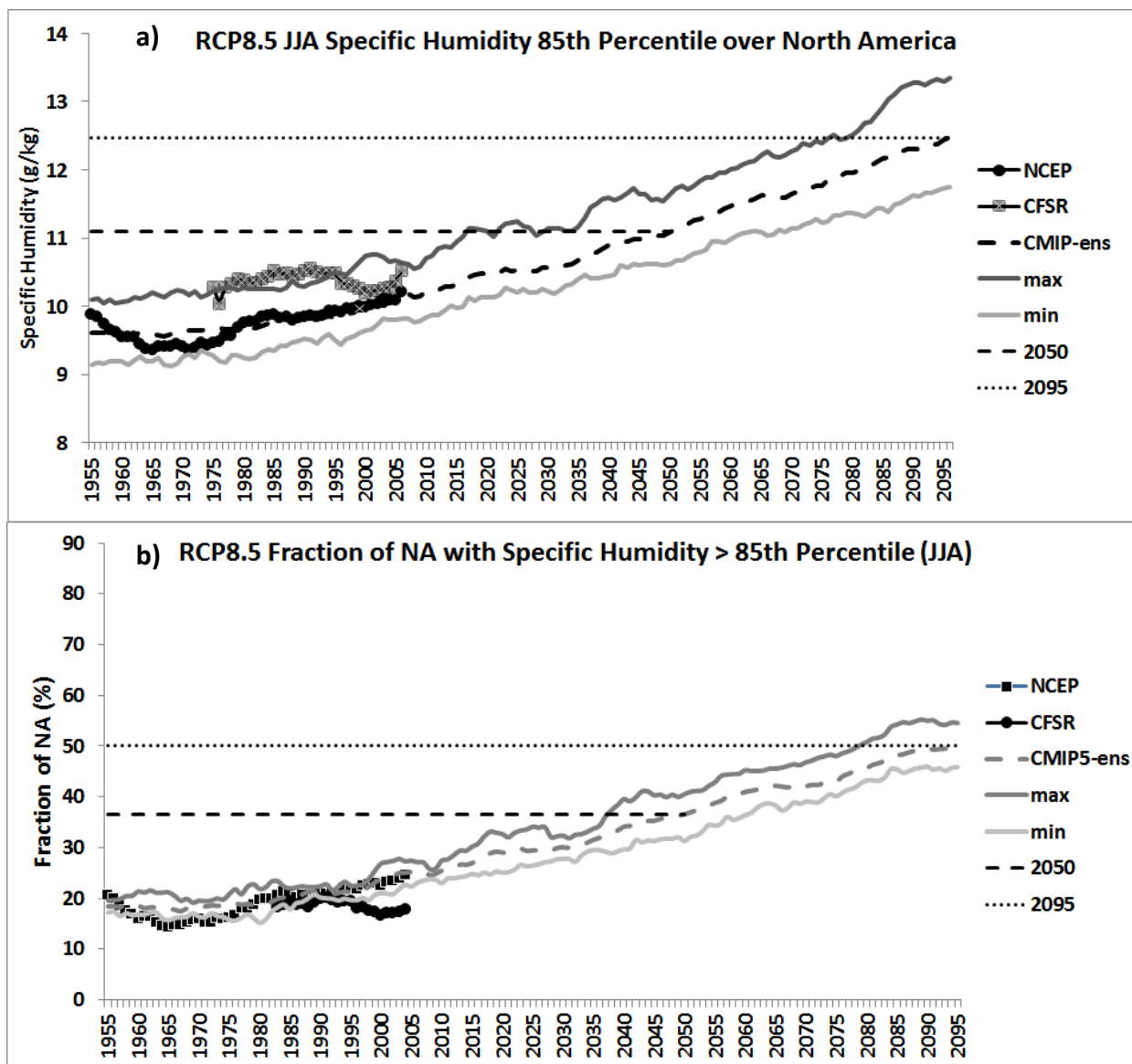


Figure 16